Abstract

Mahadevan, Pradeep. Analysis of Layer Development and Fusing for 3D Laser Printing. (Under the direction of Dr. Denis Cormier and Dr. Ola L. A. Harrysson.)

The purpose of this research is to analyze the layer development and fusing process of a new rapid prototyping process. The new rapid prototyping process is 3D laser printing, and this process is under development by researchers at the Department of Industrial Engineering at North Carolina State University. The 3D laser printing process uses principles of electrophotography (laser printing) for layer development. The layer fusing process is achieved by temperature-pressure fusing. A fiberglass reinforced Teflon sheet is to be used as a transfer medium for the layers. The effectiveness of the layer development and fusing process are evaluated via experimentation. A material testing station was developed to simulate the 3D laser printing process, and the specimens' produced were evaluated for their creep rate and uniform fusing characteristics during the temperature-pressure fusing process. The mass-to-area ratio of the layers developed by a laser printer was evaluated for their suitability for 3D laser printing. The effectiveness of Teflon as a transfer medium was compared with paper in a laser printer. The experiments performed indicate that electrophotography can be used as an effective layer development tool, Teflon can be used as an effective receiving medium for transferring toner for layer development, and temperature-pressure fusing is capable of producing fused layers for producing parts using 3D laser printing.

Analysis of Layer Development and Fusing for 3D Laser Printing

By

Pradeep Mahadevan

A thesis submitted to the Graduate Faculty of
North Carolina State University
in partial fulfillment of the
requirements for the Degree of
Master of Science

INDUSTRIAL ENGINEERING

Raleigh

2003

Approved By:

Chair

Dr. Denis Cormier

Co-Chair	Member	Member
Dr. Ola L. A. Harrysson	**Dr. Yuan-Shin Lee**	**Dr. Thomas L. Honeycutt**

Biography

Pradeep Mahadevan was born in the city of Chennai, in the state of Tamil Nadu in the southern part of India. He was raised in Chennai, where he completed his high school education in 1994. He later joined the University of Madras for a Bachelor of Engineering in Mechanical Engineering and graduated in 1998. Following graduation, he joined Brakes India Ltd., an automotive Brake manufacturing company as a Methods Engineer.

In fall 2000, the author began his graduate study at North Carolina State University. Since that time, he has been working with Dr. Denis Cormier, primarily in analyzing the layering process and determining the material requirements for the 3D laser printing process.

Acknowledgements

I wish to thank Dr. Denis Cormier for giving me this opportunity to conduct research under his guidance. I am also thankful to Dr. Ola L. A. Harrysson, Dr. Yuan-Shin Lee and Dr. Thomas L. Honeycutt for their support and patience. I would also like to thank Dr. Harvey A West and Mr. Jason C Low for their guidance, without which my studies would not have been possible. My thanks are also due to my colleagues in the Industrial Engineering Department and friends for their motivation.

TABLE OF CONTENTS

1 List of Figures

2 List of Tables

3 Introduction

The purpose of this research is to develop materials and to investigate the layering process for a low cost alternative rapid prototyping system called 3D laser printing. This process is being developed by researchers in the Industrial Engineering Department of North Carolina State University.

Rapid Prototyping (RP) systems are used to quickly develop parts from concepts. The parts developed by RP systems provide a physical model for analyses, testing and to construct molds for cast parts. Some prominent RP systems in commercial use are Stereolithography (SLA), Fused Deposition Modeling (FDM), 3-D Printing and Selective Laser Sintering (SLS). All the Rapid Prototyping systems develop parts by depositing material in layers. The CAD information of the part to be built is used in the slicing software to get information on every layer to be deposited in the rapid prototyping systems for constructing the part.

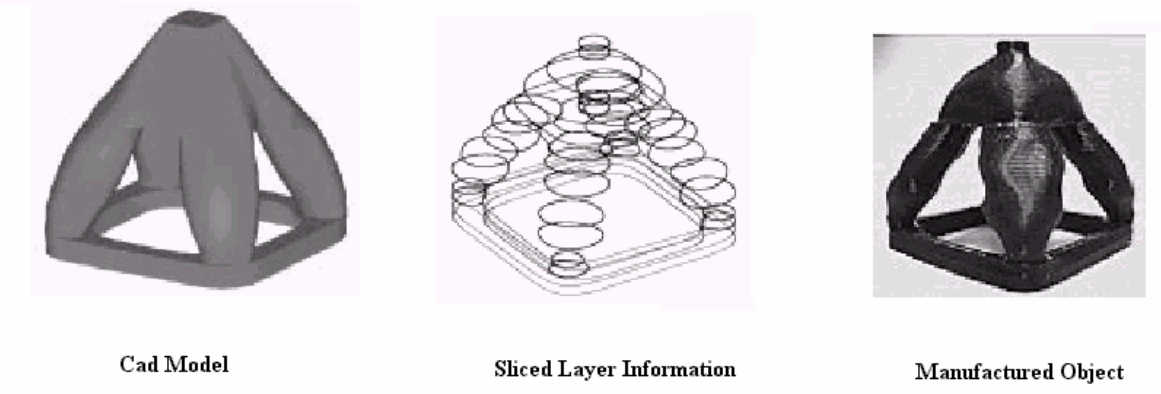

Figure 3-1 Sliced Layer Information from a Cad Model

Source: Design Laboratory, Department of Mechanical Engineering and Applied Mechanics, The University of Michigan Ann Arbor, MI.

There are certain limitations to the existing RP systems which limit their commercial exploitation. These systems are technology intensive and are very expensive to buy. The most costly RP systems can cost up to $ 800,000 and are relatively expensive to operate. RP systems such as stereolithography and solid ground curing use a photopolymer material for building parts, which limits the choice of materials. These systems also need post processing to completely cure the parts. Also many RP systems provide relatively poor accuracy and part strength.

The 3D laser printer currently under development is based on existing and perfected laser printing technology. The print engine used for depositing polymer layers is derived from a Hewlett Package laser printer. By using an existing and commercially available technology, the overall development and system costs are lowered. The process of fixing the layers takes place due to thermal diffusion by application of pressure and temperature and does not need laser curing. Also there is no post curing involved as all the layers are solidified during the process.

The materials used for the 3D printer are similar to polymer compositions already developed for laser printing and thus provide an opportunity for using a variety of thermoplastic polymer for making parts. The focus of this research is to quantify the properties of the polymer compositions and to determine the suitability of using these polymer compositions for layered manufacturing using the 3D laser printer. These advantages make the 3D laser printer a low cost alternative to existing systems.

4 Rapid Prototyping Processes

4.1 Introduction

The following sections provide a basic understanding of the working of different RP systems. This chapter also explains about the working of the 3D laser printing process and its potential advantages.

4.2 Stereolithography

The most widely used RP system is Stereolithography (www.3dsystems.com). In Stereolithography, the CAD information of the part is sliced into two dimensional horizontal cross sections with a slice thickness ranging from 0.0015" to 0.006". A laser beam is used to selectively solidify the photopolymer resin to form a layer. A wiper spreads a layer of resin to the proper thickness, and the next layer is fused by the laser beam over the previous layer. The process is repeated until the part is completed. In the case of the special Quickcast^{TM} build style, the laser beam cures the layers with an internal honey comb structure. This structure traps the uncured resin. The boundary contours of the part are completely cured by repeated passes made by the laser in a pattern of overlapping lines called skin-fill. The final curing of the part is done in a post curing oven which floods the part with ultra violet light to complete the solidification process.

Advantages of stereolithography

- The parts produced can have very high accuracy in the order of 0.001"
- The process is capable of producing intricate designs with high precision, and the parts have relatively smooth surfaces.

- Stereolithography was the first RP process to be introduces in the market, and it has proven to be a reliable and mature process over the years.

Shortcomings of Stereolithography

- The initial investment on stereolithography machine can be somewhat high as it uses a costly laser systems to cure the photopolymers.

- The process is limited by the use of photopolymers. Only certain types of polymers are used in the process.

- Considerable post processing is necessary.

4.3 Fused Deposition Modeling (FDM)

The Fused Deposition Modeling system (www.stratasys.com) uses the sliced horizontal cross section information of the CAD model in the same way as stereo lithography. The system has a fixtureless base, a spool containing filament material and a head that heats and deposits the filament material. The material is extruded through the head and deposited on the fixtureless foundation. The head moves around in a pattern set by the cross sectional CAD data. Material is deposited in layers where it adheres to the previous layer by thermal diffusion.

Advantages of Fused Deposition Modeling

- Fused Deposition Modeling does not require post curing.

- Various thermoplastic materials can be used for Fused Deposition Modeling.

- The operating temperatures are low at around 180-220 degrees Farenheit, providing a relatively safe operation. There is no worry of exposure to toxic chemicals, lasers or liquid polymers.

- The process uses no powder, and there is no messy clean up.

Shortcomings of Fused Deposition Modeling

- Accuracy of the part can be relatively low.

- The process is sensitive to variations in temperature and humidity.

- The process is relatively slow for building large parts.

4.4 Selective Laser Sintering (SLS)

Selective Laser Sintering (www.3dsystems.com) uses CAD data to get the slice information for forming layers. SLS uses polymers, metal and ceramic powders to form layers instead of liquids or sheet materials used in other processes. SLS system has infrared heat panels, which act to heat the powdered material just below the material melting point. A powder cartridge supplies powder material used to produce the part, and a roller to distribute the material evenly across the workspace. A thin layer of material is spread across the workspace platform, and a laser traces the pattern of the slice. The material is heated and fused by the laser beam. The laser beam is carefully modulated to assure that the surrounding material remains unaffected. The platform is then lowered and the process is repeated to construct successive layers.

Advantages of Selective Laser Sintering

- Selective Laser Sintering has the ability to work with a variety of materials including ceramic and metal powders.

- There is no need for post-curing.

- The unsintered material surrounding the part acts as a support structure for the part thereby eliminating the need for external support

Shortcomings of Selective Laser Sintering

- The process is fairly expensive.

- The parts produced have a textured surface finish

- The mechanical properties of the sintered materials are generally lower than those of fully dense material.

4.5 3-D Printing (3DP)

The 3DP process (www.zcorp.com) uses the horizontal cross sectional sliced data from the CAD models. A uniform layer of powder material is spread across the bed by mechanical means over a build platform. An inkjet head sprays a special binder in a specific region based on the cross sectional details of the layer. The binder binds the particles in the layer together. The same process is repeated for every layer. Layer thicknesses of 0.003"-0.010" are achieved using the Z-Corp 3-D printer. The same powder material is used as a support material for developing layers.

Advantages of Z-Corp 3-D printer

- The printing system is less expensive compared to most other RP systems.

- The build material used for making parts is less expensive.

Shortcomings of Z-Corp 3-D printer

- The parts produced have poor strength
- The process is less accurate compared with other RP processes such as stereolithography and solid ground curing.

4.6 Laminated Object Manufacturing (LOM)

Although LOM is no longer commercially offered, it is a well-known RP process. The process uses the horizontal cross sectional sliced data from the CAD model. A laser is used to cut the slice out a layer of material being used to produce the model. Once the layer is cut and deposited, another layer is cut to a suitable profile based on the slice information and deposited over the previously deposited layer. LOM uses thin sheets including paper, plastic and composite. The sheets are coated with heat sensitive adhesive, which enables the sheet to be bonded layer by layer by hot compression to form a part.

4.7 Solid Ground Curing (SGC)

Solid Ground Curing is another well-known RP process that is no longer commercially available. The SGC process used the slice data similar to rest of the rapid prototyping systems. This process has two operations that take place simultaneously to construct every layer. The first operation is the masking process in which a mask plate is electro statically charged and an image is developed on the plate using electrostatic toner to produce a mask of the slice. The second process which takes place is that of the model grower in which a thin layer of liquid polymer is spread over the work piece area. When the mask plate is ready and positioned over the workspace, a shutter is opened and a strong flash of ultraviolet light is exposed to the mask. The areas of the layer exposed to the light are cured, thus forming a solid layer of resin in the pattern of a mask. On the

work piece, all the non-solidified material is wiped off and collected for reuse. The mask plate is then cleaned of the pattern and a new image is charged on the plate. Melted wax is then used to fill the cavities of the model after the photopolymer is removed. A cooled plate is lowered on the work piece to instantly solidify the wax forming a support structure for the model. The work piece is passed under a milling cutter, which produces the layer to precise thickness and forming a flat surface to deposit the next layer of photopolymer. The process is repeated layer by layer to construct a complete model.

4.8 3D Laser Printing

This experimental system uses horizontal cross sectional sliced data to build parts in layers similar to all the commercially available rapid prototyping systems. The horizontal cross sectional sliced data is provided to a print engine one layer at a time. Based on the cross sectional data the print engine creates an electrostatic latent image on a photoconductor (Refer to Chapter 3 on electrophotography) and acquires polymer particles on the latent image. The polymer particles are then transferred to a flat receiving medium. The receiving medium is then positioned below the build platform. The build platform is then lowered making contact with the receiving medium and presses the receiving medium against a hot plate. The pressure applied by the build platform along with the heat supplied by the hot plate binds the particle to the build platform and creates thermal diffusion between particles forming a flat layer. The same process is repeated to deposit subsequent layers where the polymer particles undergo thermal diffusion within themselves and with the previous polymer layers deposited on the build platform. The polymer particles used in the process have little variation in their size and shape, which is essential for controlling the layer thickness. The final layer thickness deposited is controlled by the particle size and shape along with the pressure, temperature and time for fixing.

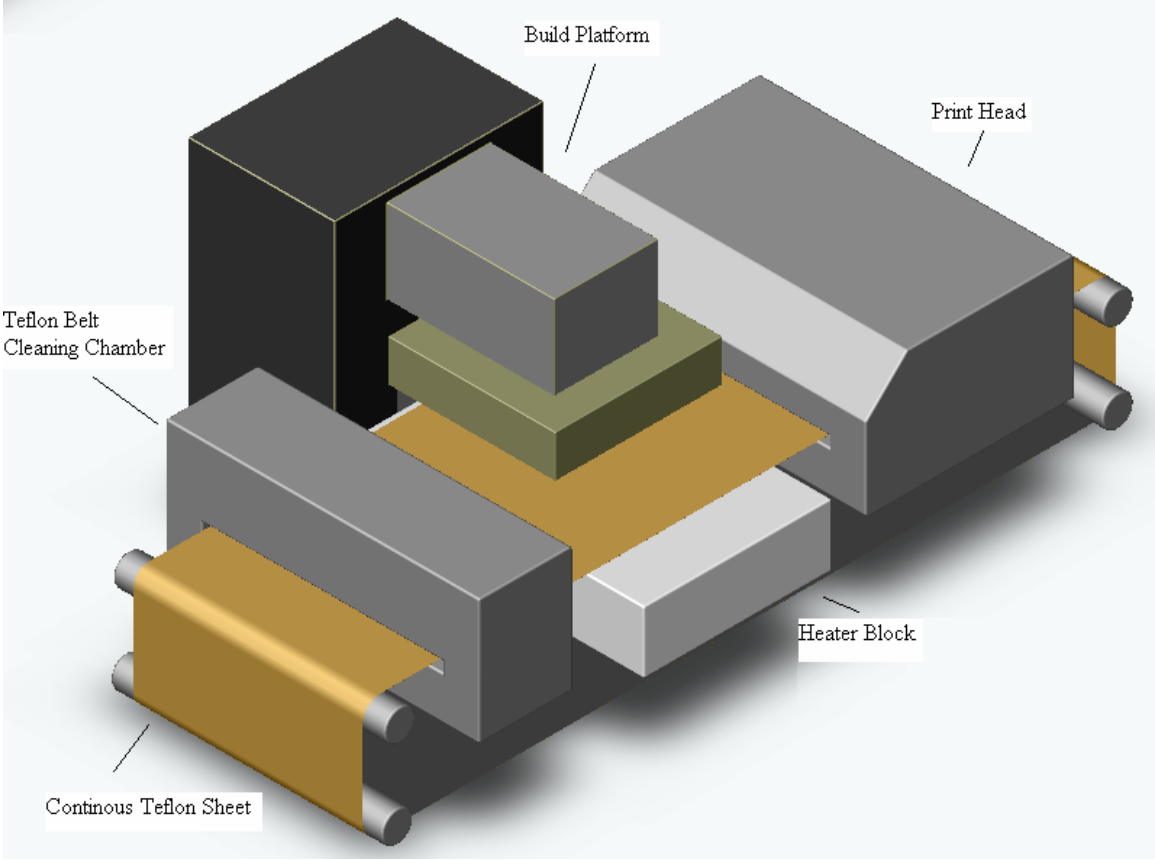

Figure 4-1 3D Laser Printer

4.8.1 Advantages of 3D Laser Printing

- The 3D laser printer is being developed using existing laser printing technology. Hence, the print engine used in the 3D laser printer will be comparable to the cost of a laser printer.

- The polymer powder materials used in a 3D laser printer are very similar to the toner used in a laser printer. There are existing methods for manufacturing and classifying polymer powder materials. The same properties measurement methods applied to the toner can be applied to the polymer powder materials. This considerably reduces the development cost of materials.

- The layer transfer from the print engine to the fixing area is done using a Teflon belt and the fixing process itself is done using a simple contact type heater block. The simplicity of the fixing process considerably reduces the cost of the RP system.

- Superior mass to area ratios are achieved by the laser print engines in every layer deposited.

4.8.2 Disadvantages of 3D Laser Printing

- The layer is fixed over the previous layers by heating the deposited layers near to polymer powder glass transition. The parts therefore undergo thermal deformation.
- Additional print engines have to be provided to provide support layers.

4.9 Summary

The different rapid prototyping processes were explained along with the newly developed 3D laser printing process. The 3D laser printer is developed mostly based on available and proven technology. The potential advantages of the 3D laser printing process can be appreciated from the above discussions.

5 Electrophotography

5.1 Introduction

As mentioned previously, the 3D laser printer is based on principles of laser printing, and an understanding of electro-photographic principles is essential to appreciate the suitability of the laser printing process for layered manufacturing. There are different types of mechanisms available for polymer powder transfer in electro photography. The material composition and properties are based on the type of transfer mechanism. The different transfer mechanisms are discussed in detail in the following sections along with the illustration of the electric fields present during toner transfer. Multilayer toner transfer feature is illustrated in the analysis of the electric field, which can be applied to attain a wide range of mass to area ratio of toner in a given layer.

There are six processes involved in producing an image using electrophotography. They are photoconductor (PC) charging, image exposure, image development, image transfer from PC to paper, fusing or fixing the paper and cleaning the photoconductor (Schein, 1992). These six steps are explained in detail in the following sections.

5.2 Photoconductor Charging

The first step in the electrophotographic process is the deposition of a uniform charge on the photoreceptor surface. This is accomplished by the corona discharge device. The corona discharge devices are comprised of a series of stainless steel or tungsten wires. The corona wires are maintained at a potential of 5 to 15 KV. The field at the vicinity of the corona wire is sufficiently high and the electrons in the region of the wires will be accelerated to velocities such that ionization of the gas molecules will occur. The positive coronas are hydrated protons of the generalized formula $(H_20)_n H+$, where n=4-8 and the negative coronas are CO_3^- . The corona discharge usually has non uniformities. To avoid

this, auxiliary electrodes are provided in close proximity to the corona, which uniformly charges the photoconductor (Borsenberger, and Weiss, 1998).

5.3 Image Exposure

The latent image formation in a laser printer is done with an infrared laser. Latent image formation typically requires an exposure between 5 - 20 ergs/cm^2. The latent image exposure with the laser creates an electron hole pair in the photo generation layer of the photoreceptor. The pair separates and is displaced to the free surface and the substrate electrode (in the photo conductor). The hole moves through the transport layer above the photo generation to the free surface and the electron moves to the substrate electrode at the bottom of the photo generation layer. The surface charge is thus dissipated to the exposed region by the hole and an electrostatic charge pattern is created.

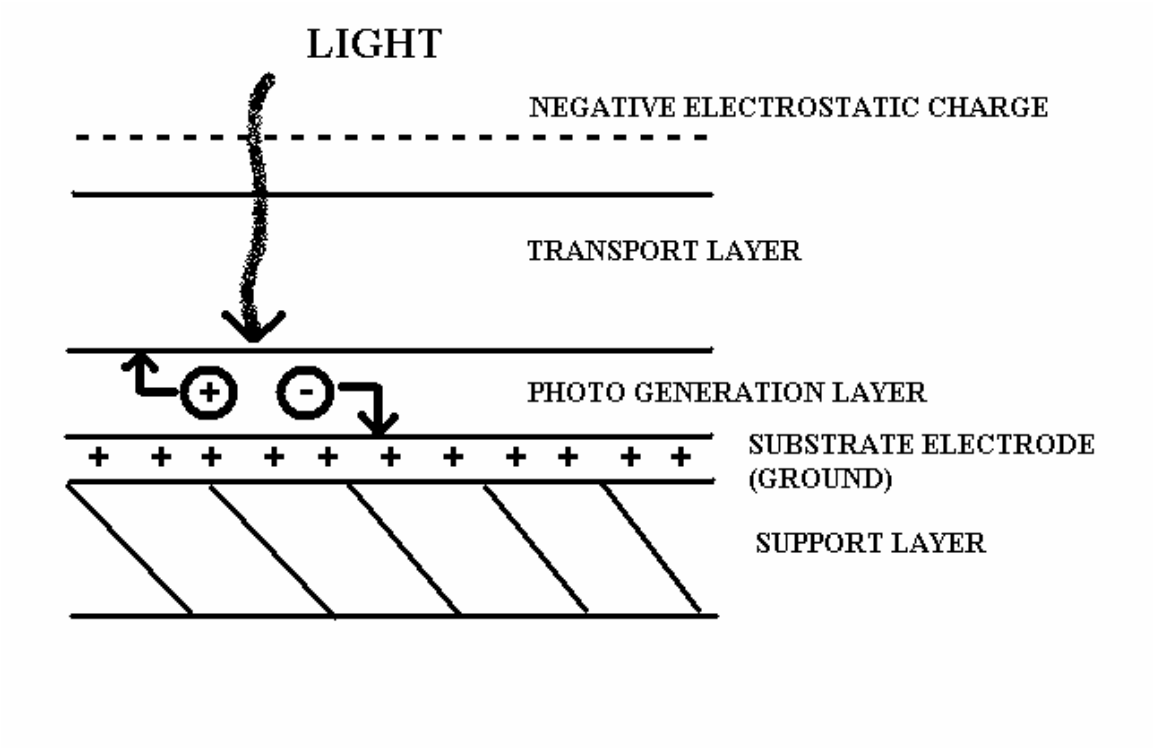

Figure 5-1 Photoconductors Used In Electrophotography

Source: Electrophotography and Development Physics by L.B. Schein (1992), Springer-Verlag Berlin Heidelberg New york publication

5.4 Image Development

In the development stage, charged toner particles are deposited on the photoreceptor. The toner particles are polymer based particles having carbon black as a colorant and for controlling the conductive properties. Magnetic properties in the toner particles are obtained by adding magnetite to the polymer during the toner manufacturing process. The toner particles are charged by triboelectrification or by corona charging to the right polarity. There are two types of image development processes. They are Charged Area Development (CAD) and discharge area development (DAD). In CAD, the toner particles are attracted to the charged area of the PC. This requires that the polarity of the toner particles be opposite to the latent image polarity of the PC. In DAD, the toner polarity is same as the photoreceptor surface and the toner particles are repelled from the charged region and deposit in the discharged regions. There are various mechanisms for toner charging and transfer. These will be explained in latter sections.

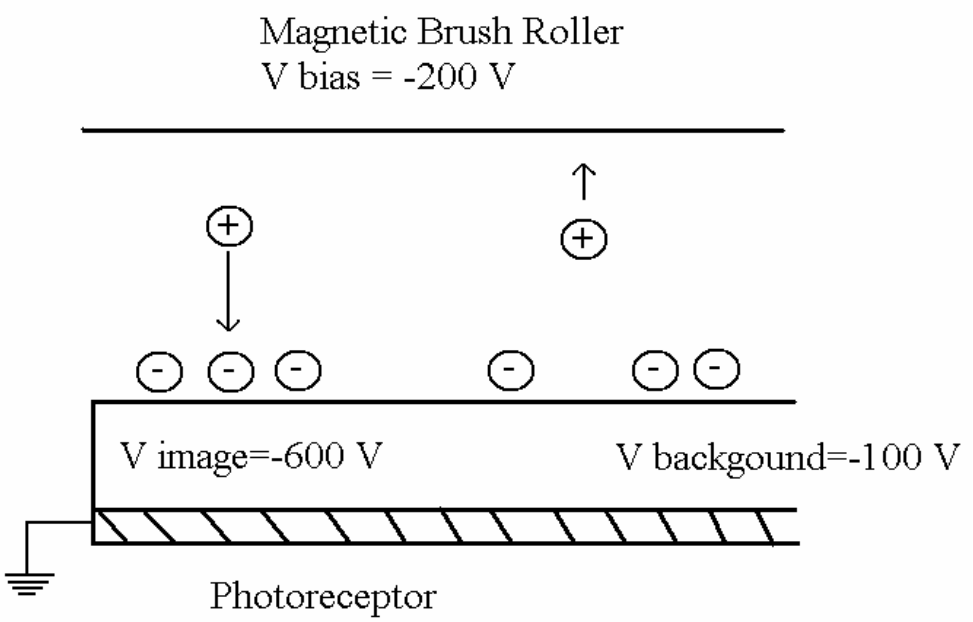

Figure 5-2 Charged Area Development Process

Source: Electrophotography and Development Physics by L.B. Schein (1992), Springer-Verlag Berlin Heidelberg New york publication

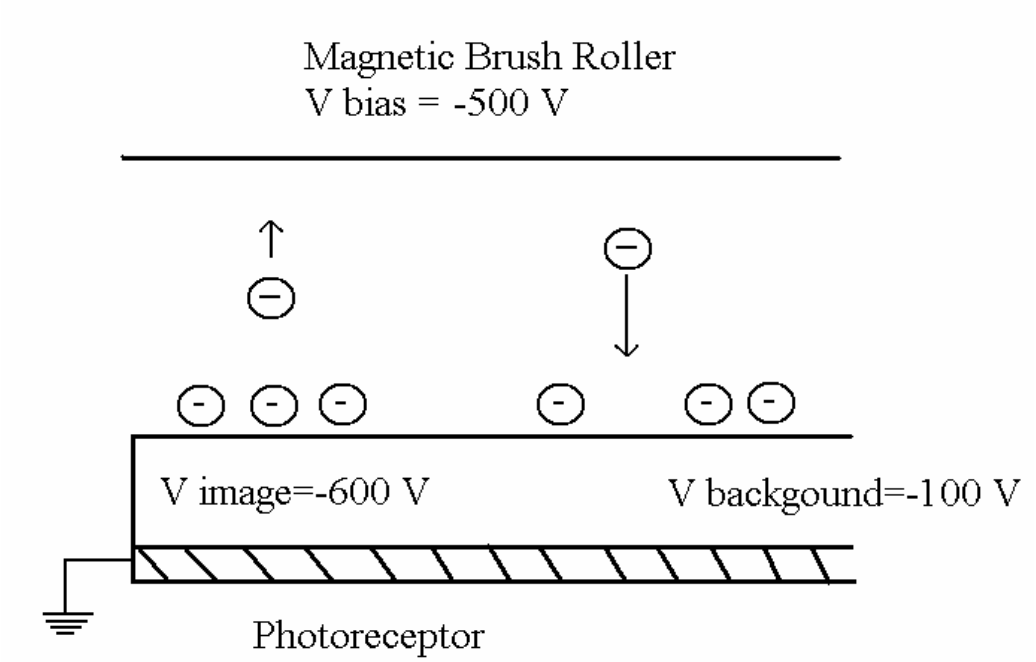

Figure 5-3 Discharged Area Development Process

Source: Electrophotography and Development Physics by L.B. Schein (1992), Springer-Verlag Berlin Heidelberg New york publication

5.5 Image Transfer From PC to Paper

After the image development process, the latent image regions are occupied by toner. The toner in the photoconductor is then transferred to a receiver medium, which is generally the paper used for laser printing. The paper is uniformly charged to the opposite polarity of the toner particles by using a corona device. For maximum contact, there must be physical contact between the toner image and the paper. The transfer of toner from the PC to the paper is usually between 85%-95%. Thus the density of the transferred image is slightly less than the density of the toner in the latent image. Toner transfer occurs when the forces on the toner due to the fields from the charge on the paper exceeds the forces between the toner and the photoreceptor.

5.6 Image Fusing

After the toner particles are transferred to the paper, the toner is fused to form a permanent image. This can be accomplished by pressure, heat and radiation. A cold pressure process is used for low volume applications and produces a lower image quality than the hot-pressure process in which a combination of pressure and temperature is used. In radiant fusing, heat generated from a quartz lamp or heated coil is used to melt the toner into the paper. The basic limitation of radiant fusing is the time required to fuse the toner. In the hot pressure process, a hot-roll pressure device is widely used. A hot-roll pressure device has a hollow roller heated internally by a quartz lamp. Oil wicks are used on the surface of the roller to prevent offset of toner on the paper.

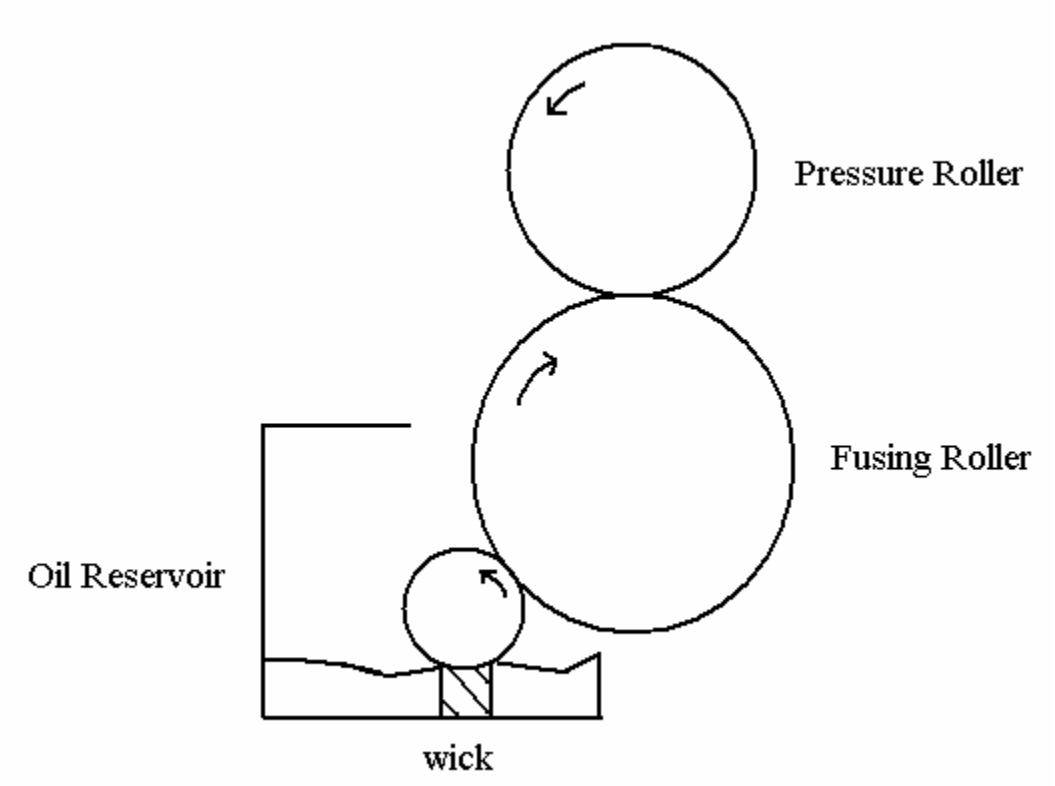

Figure 5-4 Hot Roll Pressure Fusing Device

Source: Electrophotography and Development Physics by L.B. Schein (1992), Springer-Verlag Berlin Heidelberg New york publication

5.7 Cleaning the Photoconductor

After the image transfer from PC to paper, all the residual charge in the PC must be removed along with the residual toner. Light to discharge the photoconductor or AC coronas are generally used for removing the residual charge. A brush cleaner with a vacuum system and filter is usually used to wipe the excessive toner.

5.8 Toner Transfer in Electrophotography

The various processes involved in electrophotography were explained in detail in the above section. There are different mechanisms for transferring toner to the electrostatic latent image in the photoconductor. The properties of the toner are based on the type of toner transfer mechanisms. The different toner types and their transfer mechanisms are explained in detail in the following sections.

5.8.1 Two Component Toner Transfer

Two component toner development systems have two powders, the toner and carrier mixed together. The toner particles are approximately 10 micrometers in diameter and are blends of polymer and carbon black particles. The carrier particles are approximately 200 micrometers in diameter and are composed of magnetically soft cores that are coated with a thin polymer coating. The toner and the carrier particles are charged by triboelectrification when mixed together. Depending on the materials selected for toner and carrier, the resultant charge obtained may be positive or negative. The magnitude of the charge on toner particles depends on their size and shape of the particles.

The toner is usually made from polymers such as polystyrene, polyacrylics, polymethyl methacrylate, etc. and is loaded to 10% by weight with carbon black. Carrier particles are coated with polytetrafluroehtylene, poly(vinylidene flouride), etc. The charging between the toner and the carrier particles takes place with no electric field generated over macroscopic distances, due to the size of the toner particles. This significantly reduces the probability of air discharge (Schein, 1992).

There are different mechanisms available for two component development. The development mechanisms are cascade development, insulative magnetic brush development and conductive magnetic brush development. The development methods are explained in detail in the following sections.

5.8.1.1 Cascade Development

The cascade development was invented by Battelle –Haloid development system (Schein 1992). In this development, the carrier beads and the toner are literally cascaded down the photoreceptor under the influence of gravity. The interaction of the toner with the latent image literally depends on the cascading bead velocity and bounce rate (Genthe, 1975). The development also depends on developer flow rate, developer zone angles (the angle of photoreceptor with respect to gravity), carrier properties (type, diameter, coating), toner properties (type, size, charge and concentration) and the bias electrode spacing across the photoreceptor. Based on the bias electrode across the photoconductor, the cascade development can be classified into three types as open cascade method with no electrode, conventional cascade with an electrode above the photoconductor and inverted cascade with an electrode beneath the photoconductor.

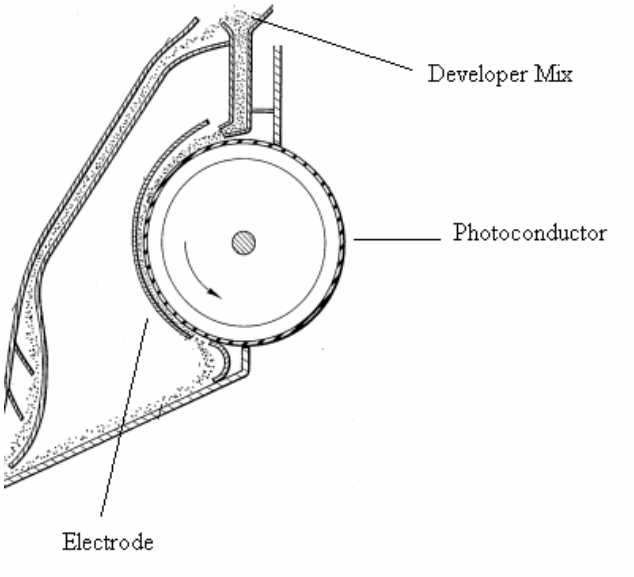

Figure 5-5 Cascade Development

Source: (1975)Itek Corporation, Lexington, Massachuset

The electrode is used for solid area development, which is a uniformly charged latent image. Without a counter electrode, the only electric field available above the photoreceptor is associated with the fringe field at the edges of the solid. Inside the latent image, there is no electric field and the toner is not attracted in these areas.

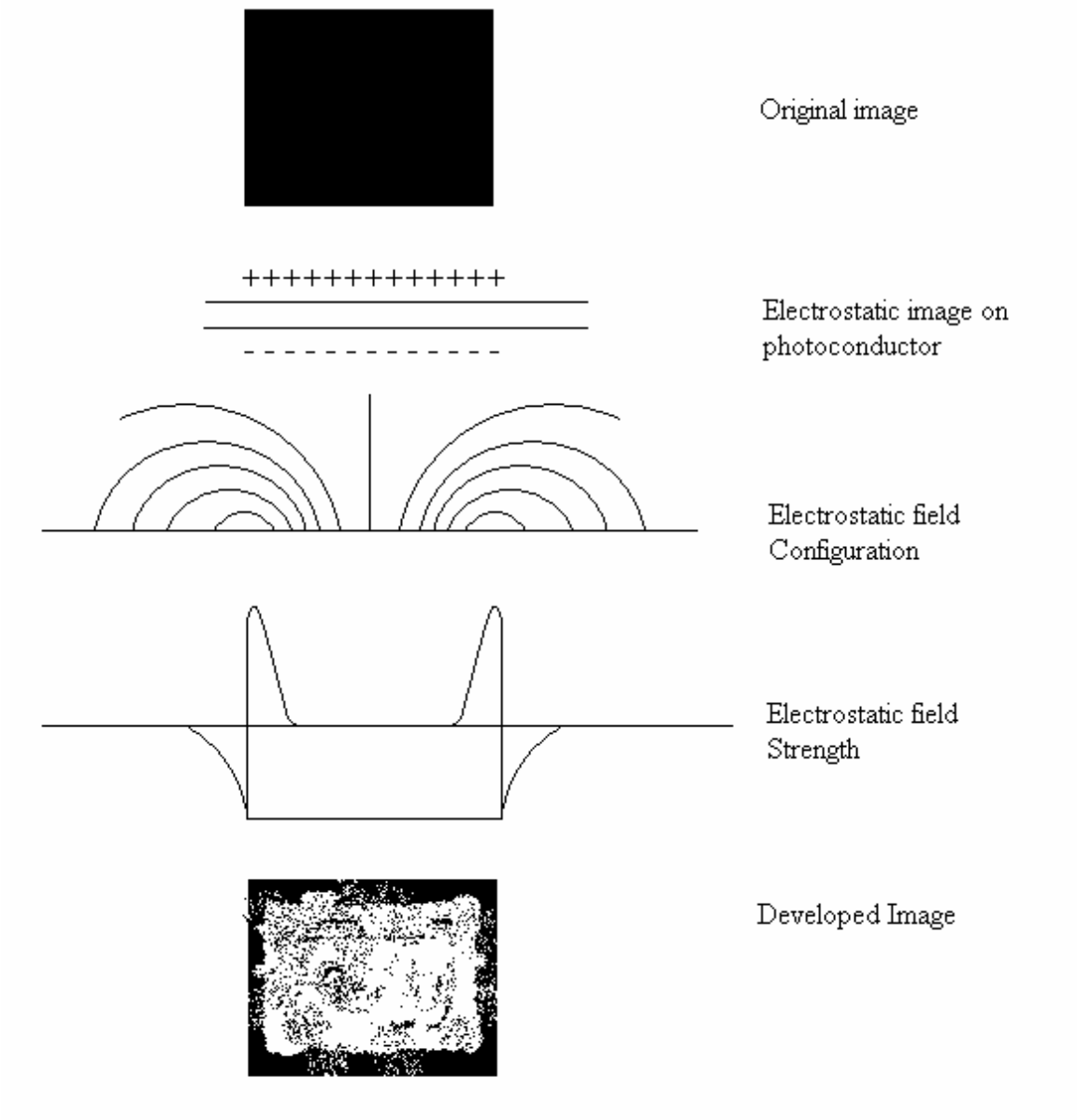

Figure 5-6 Solid Area Development

Source: Electrophotography and Development Physics by L.B. Schein (1992), Springer-Verlag Berlin Heidelberg New york publication

The theory of two component development can be further classified into airborne development and contact development. It is envisioned in airborne development (Sullivan and Thourson, 1967) that the toner is stripped from the carrier at a remote location from the image by impact of a carrier bead with another carrier bead, photoreceptor or the electrode. There are significant approximations made to the mass per unit area of the toner deposited by this model, and significant parameters are missing from this model. In contact development, the source of toner to the photoconductor is from the contact of toner and carrier with the photoconductor. The importance of the impact of the carrier bead in the presence of an electric field was clearly demonstrated by Donald and Watson (1970) in a measurement of efficiency of the toner release from carrier dropped at a fixed height. With no electric field, the efficiency was low and increased with drop height. The release efficiency is increased by a factor of 5 for a field as low as 0.1 V/micrometer.

5.8.1.2 Insulative Magnetic Brush Development

In an insulative magnetic brush development system (Schein 1992), the soft core carrier beads and the non magnetic toner mixture is introduced into the roller housing stationary magnets. The frictional force between the roller surface and the carrier beads makes the carrier move around with the roller. In the gap present between the roller and the photoreceptor, the toner particles migrate from the carrier beads on the roller to the photoreceptor surface. There are many parameters involved in the development process such as photoreceptor velocity, roller velocity, developer flow rate, photoreceptor and roller spacing, photoreceptor potential, roller bias voltage, toner properties (radii, concentration and charge to mass ratio), carrier properties (radius, shape and coating), stationary magnet strength and configuration, number of rollers, roller size, roller surface properties, photoreceptor properties (type, thickness and dielectric constant), relative humidity, dark decay, angle with respect to gravity, and reservoir capacity. The three theories suggested for solid area development are field stripping theory, powder cloud theory and the equilibrium theory.

5.8.1.3 Field Stripping Theory

In the field stripping theory, the Coulomb force $Q_t E_{air}$ (Q_t – toner charge, E_{air} – Electric field) overcomes the electrostatic image forces and Vader walls forces on the toner that attracts the toner to the carrier beads (Williams 1984). All the particles whose adhesion force is less than $Q_t E_{air}$ is developed from the carrier bead on to the latent image. According to this theory, toner particles with lower charge develop first, so the developed charge to mass ratio of the toner must increase with applied voltage. The developed mass per unit area must be linear with the toner concentration and roller velocity for a constant toner charge to mass ratio (Williams 1984) because development should increase as the amount of available toner increases. According to this theory, the developed mass per unit are is given by

$$\frac{M}{A} = \frac{2}{3} C_t \rho_C R p \nu \left(1 - \frac{1}{48\pi\varepsilon_0} \frac{Q_t}{r^2 E_{air}}\right)$$

C_t - Ratio of toner mass to carrier mass

ρ_C - Density of the carrier

R - Carrier radius

p - Carrier surface packing

ν - Ratio of roller velocity to photoreceptor velocity

ε_0 - Permittivity of free space

r - Toner radius

Q_t - Toner Charge

$\frac{M}{A}$ - Developed toner mass per unit area

5.8.1.4 Powder Cloud Theory

In powder cloud development theory (Van Engeland, 1979), the toner is freed from the carrier by inertial forces due to carrier-carrier and carrier-photoreceptor collision. The electric field associated with the latent image then attracts the toner particles. According

to this theory, the developed toner mass per unit area depends on the product of the carrier flow and the function of inertial forces on the carrier beads (Schein, 1992). The flow of the carrier particles is proportional to the roller velocity, and the inertial forces on the carrier beads increase with roller velocity. As a result, the development mass per unit area shows a linear dependence on roller velocity. If development of toner depends on the voltage applied, the developed mass per unit area must show a linear dependence to voltage. If the amount of toner is freed from the inertial forces alone, then the charge to mass ratio should be independent of the electric field. If the release of the toner depends on the inertial forces as well as toner charge, then a more complicated behavior is expected. There are two observations that confirm the existence of this theory. First, as the distance between the photoreceptor and the roller is increased, development decreases and becomes constant at a gap above 6mm, where contact between the carrier and the photoreceptor never occurs. Second, in this region of large gap, the observed current to the photoreceptor ground plane exhibits an exponential dependence, as one would expect for a dynamic process like powder cloud or field stripping.

5.8.1.5 Equilibrium Theory

Equilibrium theory (Schein, 1975) assumes that toner continues to come out of the carrier beads until the coulombs forces of the latent image balances the forces of attraction of the toner to the carrier beads. In this theory, the usual forces of attraction of the toner to the carrier beads are ignored because it is assumed that development only occurs in three body contact events between carrier, toner and photoreceptor. In this case, the forces are cancelled to first order by similar forces between the toner and the photoreceptor (Schein, 1992). The predominant force of attraction between the toner and the carrier is due to the toner particles building up a net charge as a result of toner particles developing. If n particles develop from a carrier bead, a net charge of nQ_t builds up in the carrier. Based on the extent of development, the next set of toner particles in the carrier beads are considered for development. This leads to the prediction of M / A which is linear to V. The developed mass per unit area is linear to the roller velocity with the number of carrier particles brought into contact with the point on the photoreceptor. This theory predicts

that the development of toner is independent of the amount of toner available for a constant charge because development continues until equilibrium of forces is reached. The evidence for this theory results from the experiments on controlled magnetic brush development systems. Microscopic experiments support the assumption of toner-carrier adhesion force to be cancelled by toner-photoreception adhesion force. It can be perceived intuitively that field stripping requires a basic threshold behavior for development, and no such behavior was observed for low electric fields. The development of toner was observed to be linear over a wide range of values. One would expect that the development to be proportional to the integral of toner adhesion distribution to a value determined by the applied electric field

5.8.1.6 Electric Field for Insulative Magnetic Brush Development

It is clear from all the theories, that the electric fields drive the development of all the theories (L.B. Schein, 1992). During development, the latent image of the photoconductor has a uniform charge with a charge per unit area σ_p.

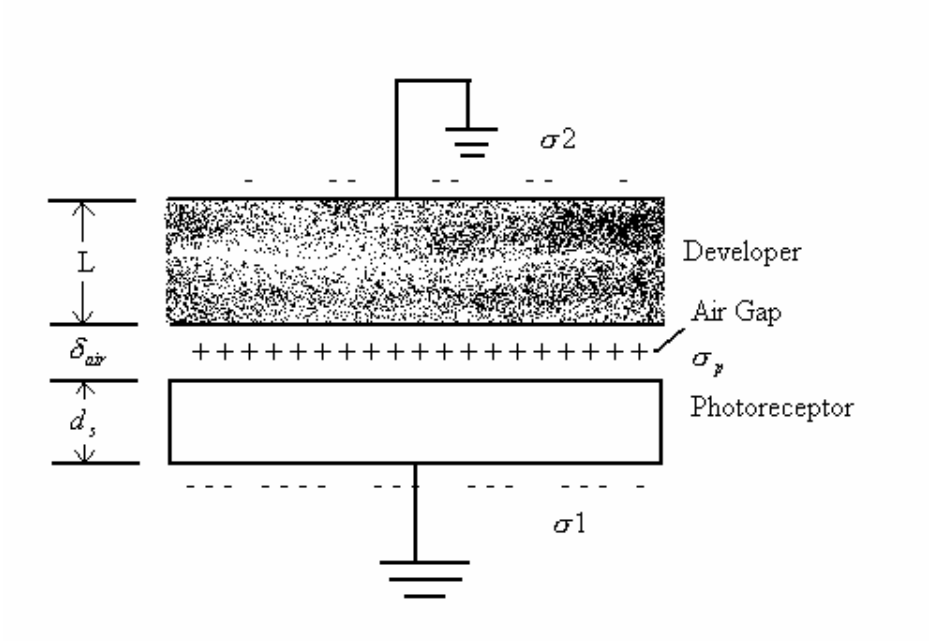

Figure 5-7 Electric Field for Insulative Magnetic Brush Development

Source: Electrophotography and Development Physics by L.B. Schein (1992), Springer-Verlag Berlin Heidelberg New york publication

The photoreceptor and the roller are assumed to be in parallel planes to determine the electric field due to σ_p. If the ground planes in the photoreceptor and the roller with a charge per unit are $\sigma 1$ and $\sigma 2$, then σ_p is

$$\sigma_p = \sigma 1 + \sigma 2$$

The electric field in the photoreceptor E_p is calculated as $\frac{\sigma 1}{K_s \varepsilon_o}$. K_s is the dielectric constant of the photoconductor, and ε_o is the permittivity of free space. The electric field in the developer, E_D, is $\frac{\sigma 2}{K_E \varepsilon_o}$, K_E is the effective developer dielectric constant. The electric field in the air gap in which the toner is trying to develop is

$$E_{air} = \frac{\sigma 2}{\varepsilon_0}$$

Since there is no voltage applied across the system, the sum of the voltage drop must be zero.

$$\frac{-\sigma 1}{K_s \varepsilon_0} \frac{d_s}{K_s} + \frac{\sigma 2}{\varepsilon_0} \delta_{air} + \frac{\sigma 2}{K_E \varepsilon_0} L = 0$$

where d_s is the photoreceptor thickness, L is the developer thickness, and δ_{air} is the small air gap in which the toner resides. The electric field in the air above the photoreceptor is

$$E_{air} = \frac{\sigma_p}{\varepsilon_0} \frac{d_s}{K_s} \Big/ \left(\frac{d_s}{K_s} + \frac{L}{K_E} + \delta_{air} \right)$$

The electrostatic potential, V, above a charged photoreceptor is defined as the potential that would be measured with no upper electrode present. This means $L = \infty$, and in this case $E_{air} = 0$, $\sigma 2 = 0$ and $\sigma 1 = \sigma_p$. The electrostatic potential V is

$$V = \frac{\sigma_p d_s}{K_s \varepsilon_0}$$

The electric field in the air gap is expressed in terms of V as

$$E_{air} = V / (\frac{d_s}{K_s} + \frac{L}{K_E} + \delta_{air})$$

During development, charged toner moves to the photoreceptor surface. The charge per unit area on the photoconductor is reduced by the presence of toner charge per unit area σ_t.

$$\sigma_t = \frac{Q}{M}\frac{M}{A}$$

where $\frac{Q}{M}$ is the charge to mass ratio and $\frac{M}{A}$ is the mass per unit area of the developed toner.

The new electrostatic field is obtained by replacing σ_p with $\sigma_p - \sigma_t$. The first order approximation (without assuming $L = \infty$) of the toner voltage V_t is defined as

$$V_t = \frac{\sigma_t d_s}{K_s \varepsilon_0} = \frac{Q}{M}\frac{M}{A}\frac{d_s}{K_s}\frac{1}{\varepsilon_0}$$

Using the above approximation, the effect of toner development on E_{air} is given as

$$E_{air} = (V - V_t) / (\frac{d_s}{K_s} + \frac{L}{K_E} + \delta_{air})$$

The second order effects are obtained by considering the toner resting on the photoconductor to have a constant volume charge density ρ_{tv}, thickness d_t and dielectric constant k_t. Using gauss law, the charged toner creates an electrostatic potential V_t of

$$V_t = \frac{\rho_{tv} d_t}{\varepsilon_0}\left(\frac{d_s}{K_s} + \frac{d_t}{2K_t}\right)$$

The above value of V_t is when $L = \infty$. The measurable parameters ρ_{tv} and d_t are expressed as

$$\rho_{tv} = (Q/M)\rho_t p_t$$

$$d_t = \frac{M}{A\rho_t p_t}$$

where ρ_t the toner is mass density and p_t is the toner volume packing. Using the above two equations, V_t can be expressed as

$$V_t = \frac{M}{A}\frac{Q}{M}\frac{1}{\varepsilon_0}\left(\frac{d_s}{K_s} + \frac{d_{t1}}{2K_t}\right)$$

The value d_{t1} is the thickness of the first monolayer developed. The value V_t is a spatial voltage, since $\frac{M}{A}$ is not continuous, being finite where the toner has developed and zero in other areas. Above the first layer of toner

$$V_t = \frac{M}{A}\Big|_1 \frac{Q}{M}\frac{1}{\varepsilon_0}\left(\frac{d_s}{K_s} + \frac{d_{t1}}{2K_t}\right) + V_2$$

$$V_2 = \frac{Q}{M}\left(\frac{M}{A} - \frac{M}{A}\Big|_1\right)\frac{1}{\varepsilon_0}\left(\frac{d_s}{K_s} + \frac{d_{t2}}{2K_t}\right)$$

Where d_{t2} is average position of the toner in the second layer and $\frac{M}{A}|_1$ is the mass per unit area of the toner developed in the first layer.

The above equations relate the voltage due to developed toner to the mass per unit area. The values d_{t1} and d_{t2} can be obtained by discharging the photoconductor by exposure to light and then measuring the remaining potential (Schein, 1992). It can be appreciated from the above discussion that it is possible to obtain a wide range of layer thickness for a given toner particle size.

$$V_t /(\frac{Q}{M}\frac{M}{A}) = \frac{d_{t1}}{2k_t}\frac{1}{\varepsilon_0}$$

$$\frac{M}{A} < \text{one monolayer}$$

$$(V_t - V_t|_1) \Big/ (Q/M)(\frac{M}{A} - \frac{M}{A}|_1) = \frac{d_{t2}}{K_t}\frac{1}{\varepsilon_0}$$

$$\frac{M}{A} > \text{one monolayer} \quad d_s = 0$$

Where $V_t|_1$ is the toner voltage at the first monolayer. Experiments were conducted by L.B. Schein in 1974 to verify the above results, and distinct observations were made on the first and second monolayer. It was observed that the electrostatic potential of the photoreceptor changes before and after development. The change was observed to be due to V_t and also due to the additional charging of the photoreceptor due to the interaction of carrier and toner with the photoreceptor. These results and experiments prove that it is possible to develop multiple layers of toner in a single development cycle and a wide range of $\frac{M}{A}$ ratio can be achieved by adjusting the photoreceptor potential.

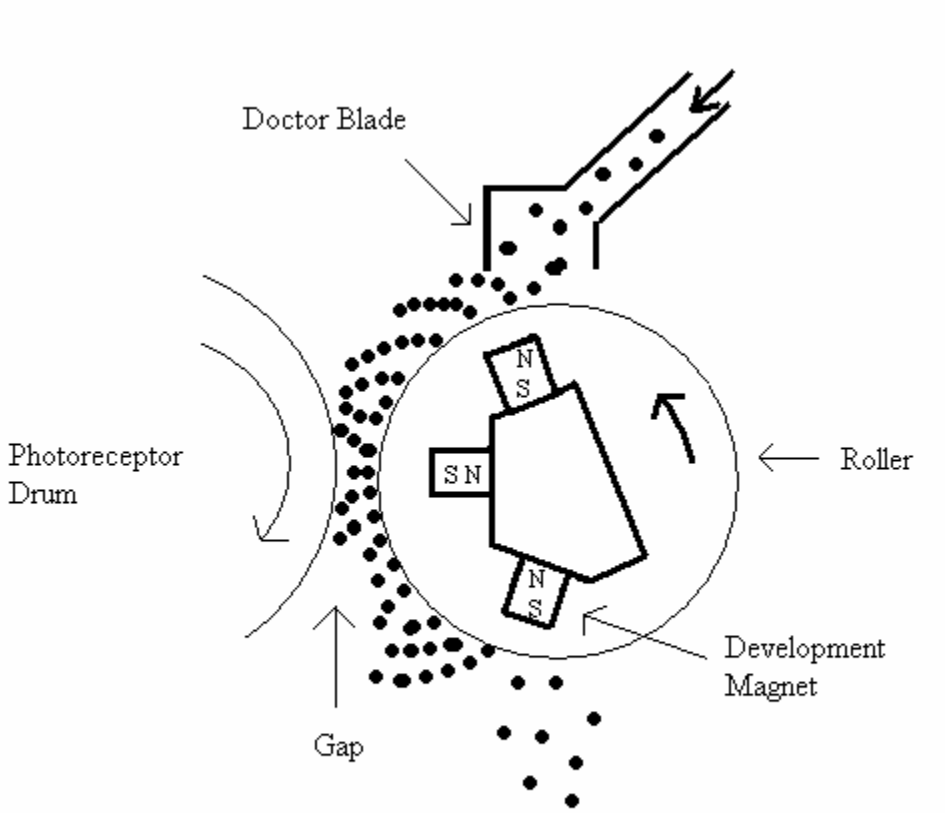

Figure 5-8 Insulative Magnetic Brush Development

Source: Electrophotography and Development Physics by L.B. Schein (1992), Springer-Verlag Berlin Heidelberg New york publication

5.8.1.7 Conductive Magnetic Brush Development

The conductive magnetic brush development (L.B. Schein, 1992) provides improved copy quality compared to insulative magnetic brush development. The conductive magnetic brush development uses a sponge-shaped carrier bead for development instead of the spherical carrier beads used in insulative magnetic brush development. The carrier particles are called sponge shaped carrier particles as their surfaces have a sponge like appearance when viewed under scanning electron microscope. The sponge shaped carrier particles provide a better conductivity path down the bead chain by eliminating the toner between the carrier beads. The development is limited for insulative magnetic brush

development because of the build up of charge on the carrier beads adjacent to the photoreceptor. The conductive path short circuits the stored charge on the carrier to the ground thereby increasing the development of toner.

5.8.2 Monocomponent Development

5.8.2.1 Induction Charging for Conductive toner

The conductive toner particles can be charged by contacting them with a metal and imposing an electric charge. The charge will flow from the metal to the particle and charge the particle. A conductive toner particle sitting on a positive electrode plate might acquire a positive charge and will be attracted by a negatively charged photoreceptor. The toner particle after migrating to the photoreceptor will lose the negative charge and acquire a positive charge and will be repelled back to the electrode plate. To avoid the bouncing of toner, the resistivity of the toner must be given careful consideration (Choi, 1964). The induction charging mechanism assumes a simple RC circuit charging model. When the charging magnetic roller rotates, the toner particles move in the opposite direction and there is a rise and fall of toner chains following the magnetic field lines. In the development zone, the toner is chained by the radial magnetic field between the roller and the photoreceptor surface, forming a conductive path. The time constant for the charge to move down the chain is $\rho K_t \varepsilon_0$. ρ is the resistivity of the chain, K_t is the dielectric constant of the toner and ε_0 is the permittivity of free space. Clearly this time constant must be less than the time the toner in the development zone. Characterization of the resistivity of toner is very difficult because it includes the interface between toner particles. The resistivity of the toner particulate system is often electric field dependent and also varies from chain to chain.

5.8.2.2 Injection Charging

In the injection charging techniques (Nelson, 1976), insulative magnetic toner is used. The toner is transported around the roller by the rotation of the roller or by the magnets inside a static roller. The insulative toner is charged by injection from the roller in the

presence of a magnetic field. The critical aspect of the invention is the turbulent mixing of the toner particles around the roller to produce uniform charging.

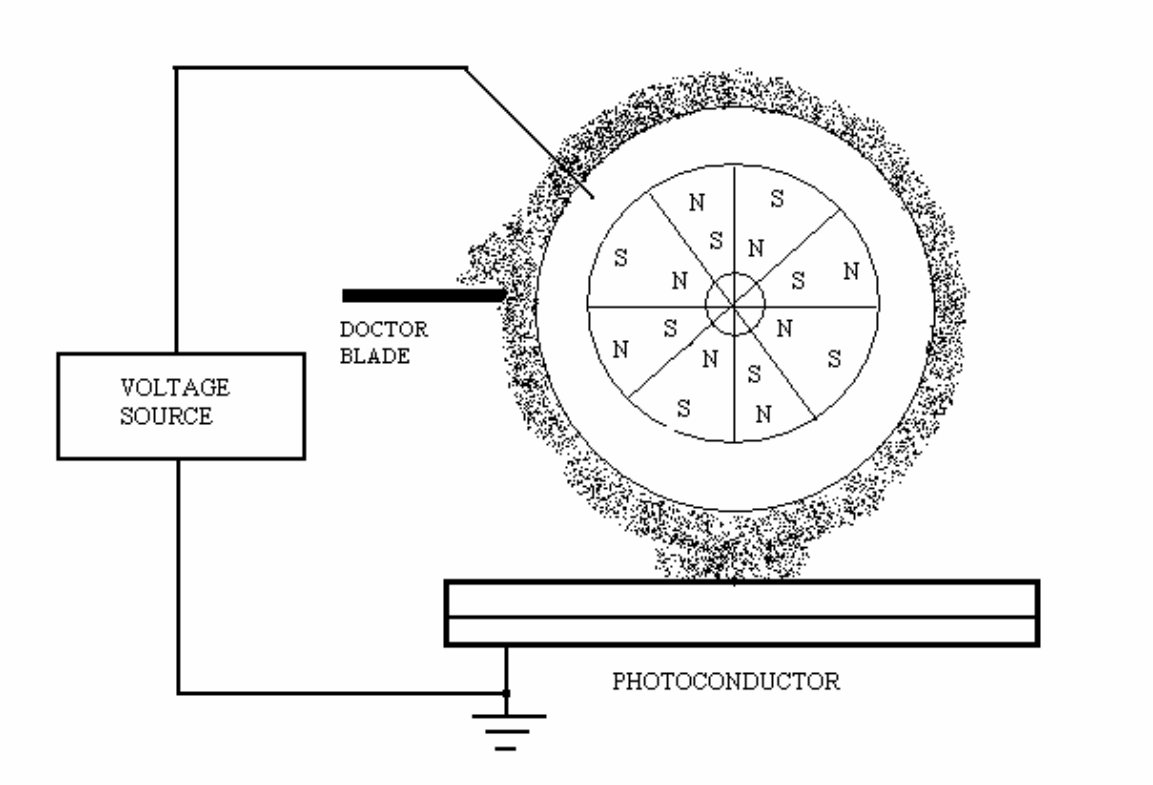

Figure 5-9 Injection Charging

Source: Electrophotography and Development Physics by L.B. Schein (1992), Springer-Verlag Berlin Heidelberg New york publication

The charge to mass ratio strongly depends on the velocity of the roller. There is an interesting theory of toner chain rotation proposed for injection charging of toner by Nakajima in 1980. It is suggested that when the roller rotates around the stationary magnets, the toner filaments form large lumps, or trees (chains) that cartwheel along the surface. As the toner chain cartwheels the end toner particles in the chain comes into contact with the roller surface and gets charged.

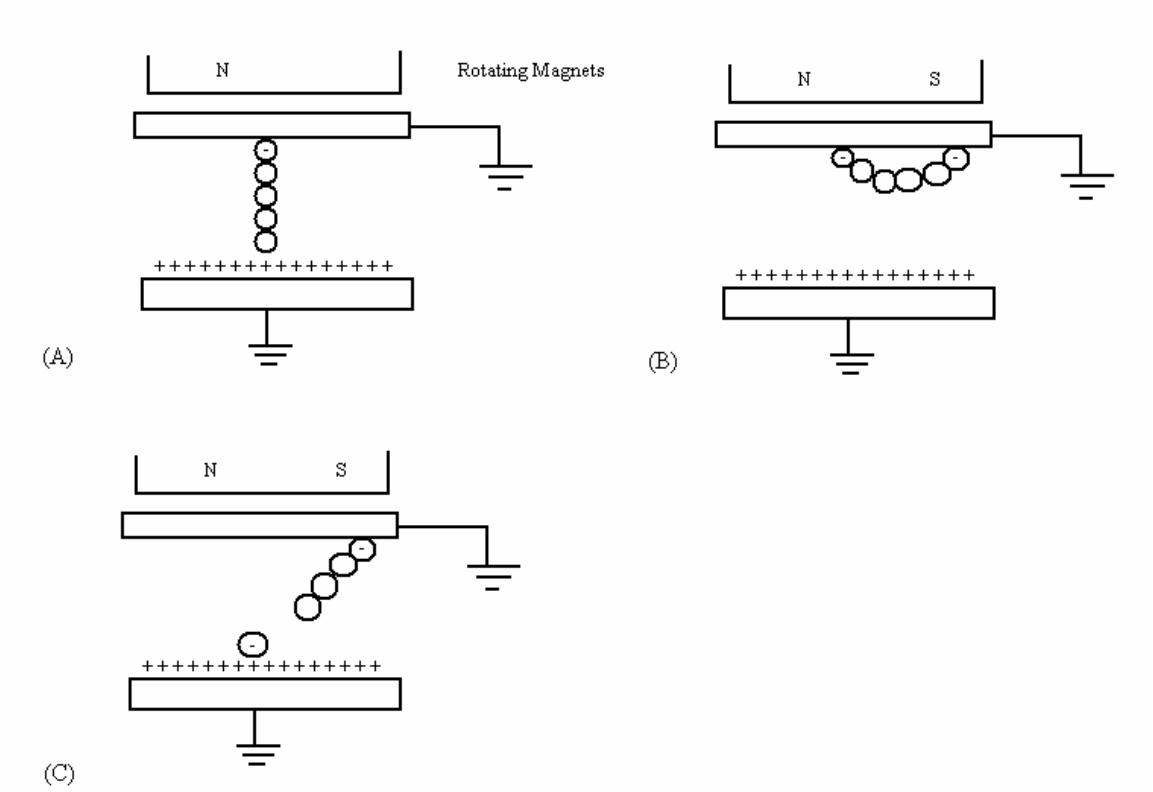

Figure 5-10 Nakajima's Model of Injection Charging

Source: Electrophotography and Development Physics by L.B. Schein (1992), Springer-Verlag Berlin Heidelberg New york publication

It was observed that different toner charging characteristics can be obtained by varying R_{dd}, defined as the ratio of the development gap to the doctor blade gap. At R_{dd}, less than 0.9 toner behaved conductively and the development is low. The interparticle conductivity is higher at R_{dd} values less the 0.9, where higher packing fraction of toner occurs. Development was observed at higher R_{dd} values above 0.9 where interparticle conductivity is low.

5.8.2.3 Contact Charging

In contact charging toner is charged by triboelectrification (Schein, 1992). A roller rotates about a stationary magnet in a reservoir of magnetic, highly insulating monocomponent toner. The toner is charged by contact with the roller surface and is carried out of the

reservoir past a magnetic doctor blade. It was proven in experiments that the toner charging is caused only due to the contact charging of toner particles with the roller surface. This was proven by changing the resin coated on the roller. The magnetic doctor blade is used to split the toner chain where the spatial derivative of the magnetic field, which determines toner-toner adhesion. A research group at Ricoh (Schein, 1992) proved that the charge on every toner particle is propotional to the square of the radius of the toner particle for radii less than 6 micrometer. Above 6 micrometer, the charge tends to become independent of radius. Another research group at Toshiba performed experiments with a special metering blade (Doctor Blade) designed to apply pressure to the roller (Schein, 1992). The toner charge and the layer thickness depends on the pressure applied. The charge to mass ratio increases with the pressure applied, and the mass to area ratio decreases with the pressure applied.

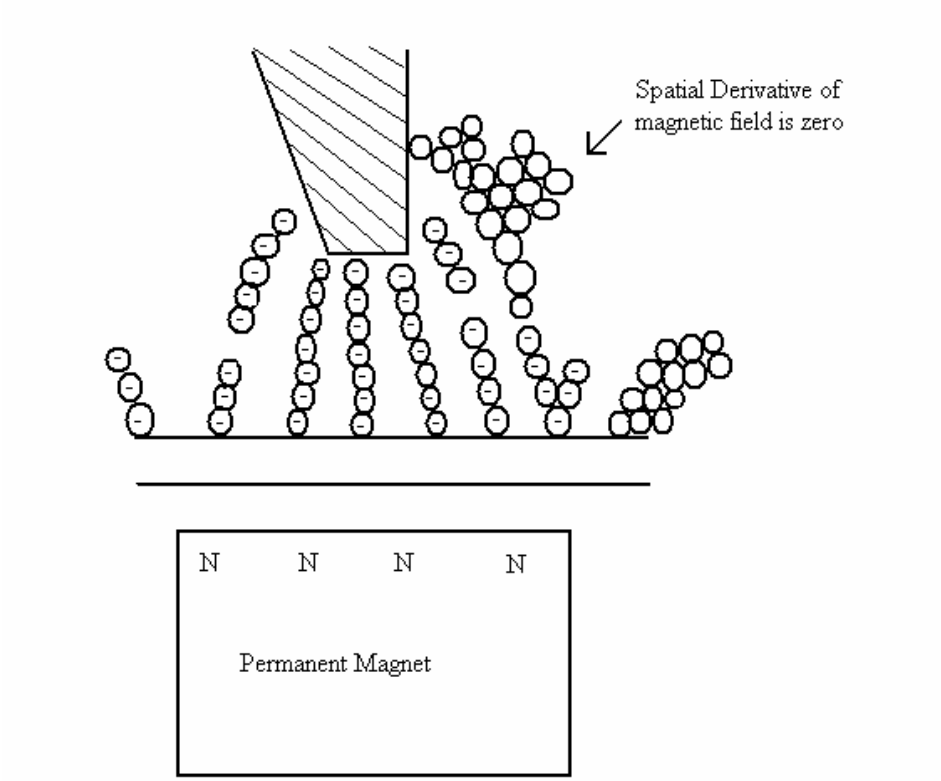

Figure 5-11 Doctor Blade used in Contact Charging

Source: Electrophotography and Development Physics by L.B. Schein (1992), Springer-Verlag Berlin Heidelberg New york publication

5.8.2.4 Corona Charging

Corona Charging can be achieved on toner by placing a corona device adjacent to the roller housing the permanent magnets (Schein, 1992). The toner is attracted by the roller, and the corona device charges the toner uniformly by ion emission. The problem with corona charging is the contamination to the corona wire by the toner particles which do not permit uniform charging of the toner on the roller surface.

5.9 Summary

The basic steps involved in image development and transfer in electro photography were explained. The transfer of toner in an electric field present in the development region was illustrated to provide an understanding of toner transfer and to prove that multilayer toner transfer is possible by adjusting the photoconductor and bias electrode voltage. The requirements for different toner transfer mechanisms in electro photography were explained along with the theory of toner charging. The purpose of a doctor blade used in contact charging, which is widely used in monocomponent toner transfer, was illustrated. This chapter provided a clear understanding of layer development using electrophotography.

6 Polymer Powder Manufacturing and Properties Measurement

6.1 Introduction

The polymer powder manufacturing and classification processes are explained in this chapter. There are polymer properties associated with the flow ability, electrostatic image development and fixing processes. The polymer properties and measurement methods are explained in detail in the following sections.

6.2 Polymer Powder Manufacturing

Toner is prepared by melting and kneading resin, magnetite particles, charge control agent and coloring agent (carbon black). The kneading is done in an extrusion machine or batch mixer. The polymer resin is melted, and the high shear in the extrusion machine causes the components to be evenly dispersed within the matrix.

The fused mixture is then subjected to coarse crushing followed by fine pulverization. The fine pulverization is done by a jet milling process. In the Jet milling process, the toner particles are carried by opposed air jets, and the fine pulverization takes place by the impact of the toner particles in the opposed jets. The particles are then carried into a separation chamber where the smaller particles with lesser mass are separated through an outlet and further collected through a filter. The larger particles are returned by the air jet into the impact chamber and are pulverized into finer particles. There are number of classifiers available with different working principles to classify and separate toner particles of the right size. The toner is then subjected to a process called speriodization (Kumar, 2000) in which the toner particles are passed in a stream of hot air to attain the spherical shape that is vital for toner flow-ability. Fluidizing agents such as hydrophilic silica are then added to the toner to improve its flow properties.

There are several limitations to the conventional toner melt kneading and jet milling processes. The dispersion of carbon black and small amounts of charge control agents are difficult. There is a problem of decomposition of charge control agent during melt

kneading. There may be excessive abrasion of iron oxide used in the mixture and the jet milling process is energy intensive (Cooper, 1992). The particle size distribution produced by jet milling is also large.

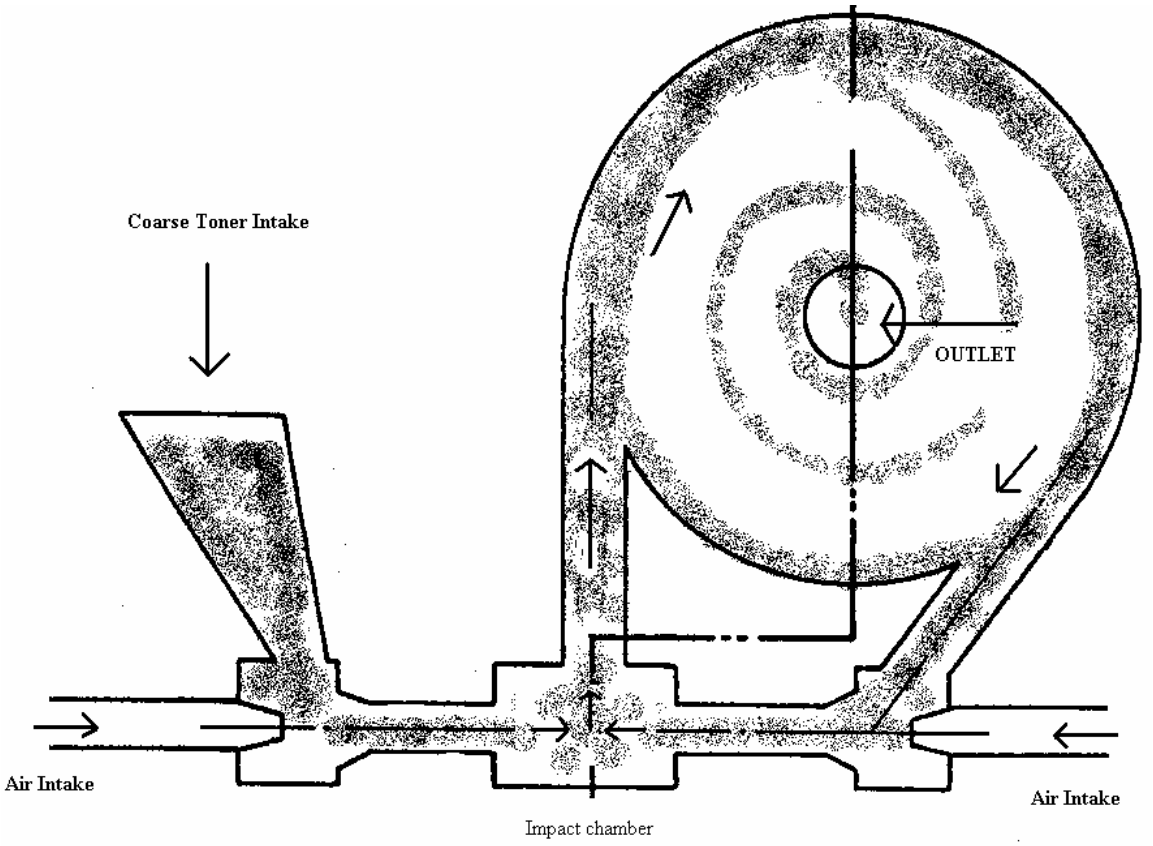

Figure 6-1 Jet mill

The alternative to melt kneading is suspension or dispersion polymerization and spray drying. In the suspension polymerization process, a mixture composed of monomer composition is added to the polymerization initiator in an aqueous medium for polymerization to take place. The polymerized particles obtained by suspension polymerization exhibit excellent flow properties because of the uniform spherical shape of the particles. The suspension polymerization process is cost effective compared with the conventional melt kneading/ jet milling process. A disadvantage with the suspension polymerization process is that the particles exhibit poor charging capabilities as the

charge control agent cannot be uniformly dispersed in the polymerized particles as in melt kneading (Kamiyama, 1993).

In the spray drying process, the toner particles are produced by interfacial polycondensation. A first non-aqueous reacting material is emulsified in an aqueous phase containing the second reacting material. The reaction between the first and second reacting materials takes place by agitation to produce microdroplets of non aqueous phase encapsulated with a substantially impervious polymeric compound. This shell produces resistance to abrasion from other particles and protects the toner particles from the effects of the environment. These types of toners are known as encapsulated toners. The substance encapsulated in interfacial polycondesation contains coloring material, magnetite of ferrite, binder for the coloring material such as vegetable oil, aliphatic or aromatic hydrocarbon solvent, antioxidants and a carrier medium comprising a solvent or a plasticizer containing the first reactive substance. The second reactive substance is an amine containing substances such as diethylene triamine with PH stabilizers like sodium carbonate. After agitation, the mixture forms a slurry and the slurry is spray dried to form discrete capsular particles (Matkan, 1980). The toner particles produced by spray drying have the same disadvantage as the particles produced by suspension polymerization.

6.3 Powder Polymer Properties and Measurements

The accuracy of a part developed using a 3D laser printer depends largely on the material properties. The layer developed must have uniform mass to area ratio and consistency in particle shape and size to attain repeatable fused layer thickness. The proper development of the latent image in the photoreceptor and subsequent transfer of the developed image to a receiving medium depends on properties such as polymer particle size and shape, charge to mass ratio and toner flow-ability. There are several measurement methods for determining the toner properties in electro photography that can be applied to powder polymer materials used in 3D laser printing. The measurement methods are described in detail in the following sections.

6.4 Triboelectrification

Toner particles get charged by a process known as triboelectrification. When two neutral surfaces comes into contact with each other and then separate, the particles will undergo tribocharging and will be at a non neutral surface charge level. The level and the polarity of this acquired surface charge depends on several factors. The mechanism of triboelectrification is explained in the following sections.

- **Surface Contact Effect**

  Surface contact effects include the surfaces roughness, contact force, and frictional heating (caused by rubbing), all of which influence the amount of surface area that is in contact with the other material during tribocharging (Allen, 2000). The greater the surface contact, the greater the resulting net charge may be when two surfaces are separated after contact.

  - The increased surface roughness between the contact surfaces results in decreased surface contact leading to reduced charging (Moriya, 1994).

  - . The uniformity in the size and shape of toner powder results in uniform charging

  - Smaller toner particle size results in increased contact surface area for triboelectrification.

- **Work Function**

  The work function is the property of a material's ability to hold onto its free electrons (the electrons orbiting the outer most shell of the material). The greater the material's work function, the less likely it is to give up its free electrons during contact (triboelectric generation). The weaker the work function is, the more likely the material will acquire a more positive charge by giving up or loosing some of its free electrons. In general, materials with higher work functions tend

to appropriate electrons from materials with lower work functions. The triboelectric series has a list of materials based on the tendency give up and acquire electrons. The triboelectric series in the following section has been determined empirically by the charge attained by the material when it comes into contact with a different material.

Table 6.1 Triboelectric Series

Source: Electrophotography and Development Physics by L.B. Schein (1992), Springer-Verlag Berlin Heidelberg New york publication

Positive
Silicone elastomer with silica filler
Borosilicate glass, fire polished
Window glass
Aniline-formol resin, acid catalyzed
Polyformaldehyde
Polymethylmethaacrylate
Ehtylcellulose
Polyaimde 11
Polyamide 6-6
Rock Salt (NaCl)
Melamine formol
Wool, Knitted
Silica, fire polished
Silk, Woven
Polyethylene glycol succinate
Cellulose acetate
Polyehtylene glycol adipate

Polydiallyl phthalate
Cellulose sponge
Cotton, woven
Polyurethane elastomer
Styrene-acrylonitrile copolymer
Styrene-Butadiene copolymer
Polystyrene
Polyisobutylene
Polyurethane flexible sponge
Borosilicate glass, ground state
Polyethylene glycol terepthalate
Polyvinyl butyral
Formo phenolique, hardened
Epoxide resin
Polychlorobutadiene
Butadiene-acrylonitrile copolymer
Natural rubber
Polyacrylonitrile
Sulphur
Polyethylene
Polydiphenyol propane carbonate
Chlorinated polyether
Polyvinyl chloride with 25% DOP
Polyvinyl chloride without plasticizer
Polytriflurochloroethylene
Polytetrafluroethylene
Polytetrafluroethylene
Negative

Charge Back Flow

Charge backflow occurs when two materials have been charged possibly from the above mechanisms and are then separated from intimate contact. The backflow of some of this charge imbalance may flow back to the original material reducing to some degree the net charge (charge imbalance) on either surface from tribocharging.

Gas Breakdown

Gas breakdown can occur between two surfaces during separation. The microscopic surface topology of a surface has many peaks and valleys. It is one of these peaks that may have substantial charge that yields a large electric field in a very small area causing corona discharge or the breaking down of the air molecules which were acting as a dielectric (insulator between the two separating surfaces). During this breakdown, charge can be transferred from one surface to the other via the path of the electrified air (plasma). The amount of charge transferred is dependent on the distance of separation and the gas pressure. This is one of the reasons for the toner particles to have shape factor (section 4.17.1) close to one.

6.5 Toner Charge Measurement

The electrostatic properties of the powder polymer can be quantified by determining the charge to mass ratio of the powder polymer. The powder polymer is charged by triboelectrification and must exhibit uniform charging properties to avoid unwanted effects like background development, where lower charge to mass ratio particles adhere to the non latent image areas. The different charge to mass measuring method are explained in the following sections.

6.5.1 Charge Measurement of Two component Toner

6.5.1.1 Toner Draw Off Charge Measurement System

A Faraday's cage is used in a toner draw off charge measurement system (ASTM F 1425-92) along with precision coulomb meters for charge measurement. The Faraday's cage

has an insulative block with a fine mesh. A mesh size is selected that retains the carrier particles and, which allows the toner particles to pass through. The sample to be measured in the Faraday's cage is prepared by mixing a suitable quantity of toner and carrier particles.

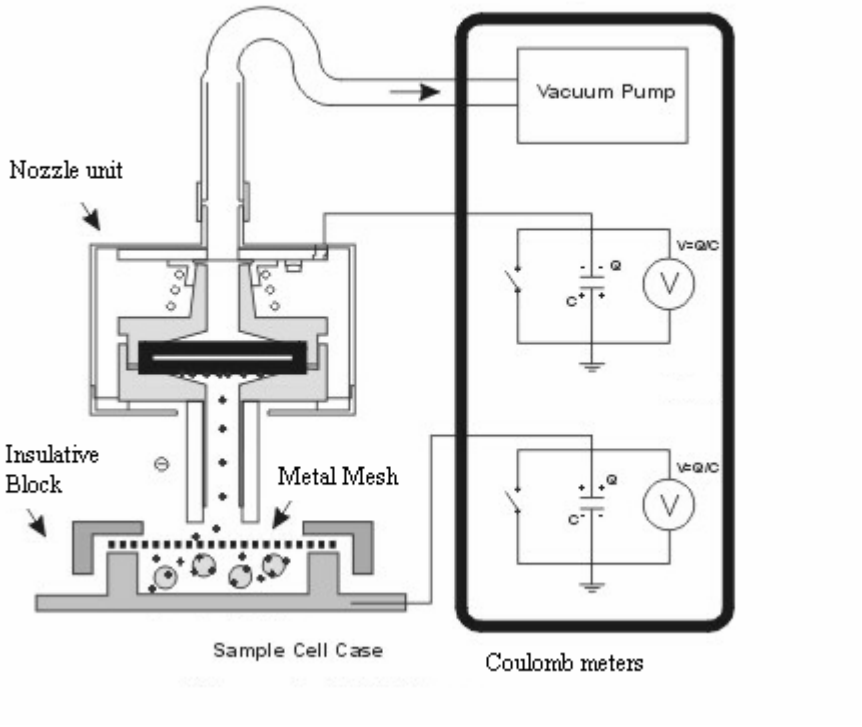

Figure 6-2 Toner Draw Off Charge Measurement

Source: Trek Inc, Medina, New York,
http://www.trekinc.com/app_note_1001/210HS_Application_note.htm

The sample is mixed by tumbling in a roller unit for thirty minutes and is transferred to the insulative block of the Faraday's cage. The sample is then covered with the wire mesh and connected to the nozzle unit. The toner particles are sucked out of the mesh by vacuum through the nozzle unit, and the carrier particles are retained in the insulative block by the mesh. The residual charge on the carrier particles are measured by precision coulomb meter. The weight of the insulative block with the mixture is measured before and after the draw off of the toner, and the charge to mass ratio is determined from the charge measurement and the toner weight loss.

6.5.2 Charge Measurement of Monocomponent Toner

6.5.2.1 Electric Field Migration Method - Zeta Sizer

In this method, the toner migration rate or particle velocity in the electric field is measured and the amount of electric charge on the toner particles is calculated. The Zeta sizer measures the light scattered from the laser beam as it passes through the suspension. In the absence of the electric field, the scattered light provides information about the particle size. If a slowly varying electric field is applied, the particle charge can be obtained from the fluctuating light signal (O'Brien, 1989) by determining the speed of the particle to the applies electric field. The shortcoming with this method is the difficulty in separating the toner particles into individual particles for measurement.

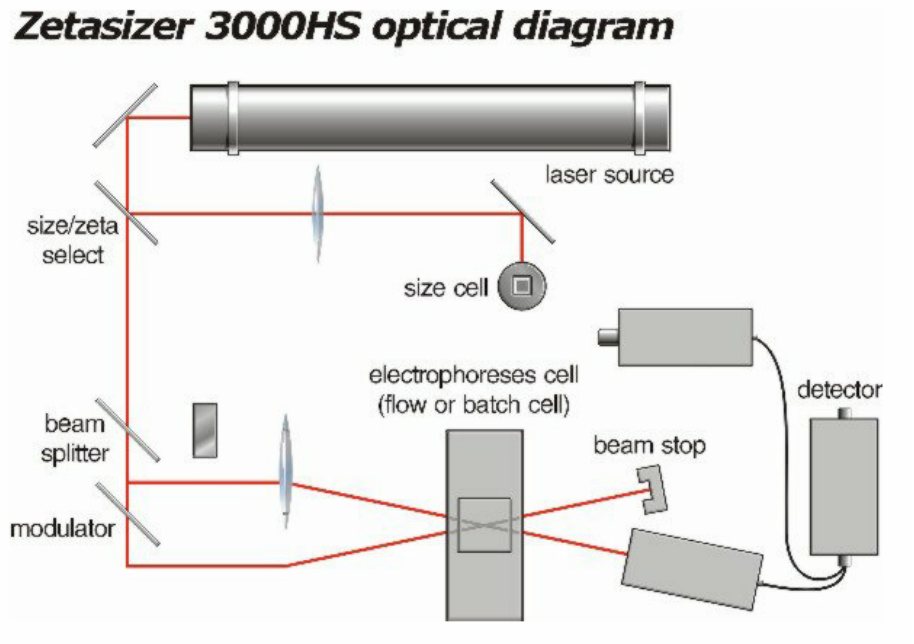

Figure 6-3 Zetasizer for Particle Size and Charge Measurement

Source: Malvern Instruments (UK)
www.colloidalsciencelab.com/ Equipment/zetadv.html

6.5.2.2 Developing Current Method

In this method, the migration of the electric charge during development is measured as an electric current and the amount of electric charge of the toner particles is calculated. The

disadvantage with this method is that the measurement is affected by noise and loses stability (O'Brien, 1989).

6.5.2.3 Surface Potential Method

In the surface potential method, the toner is allowed to develop in a photoreceptor plate. After development, the charge on the photoreceptor is neutralized and the residual charge on the toner is measured for a given area using coulomb meters and accessories used for measuring surface potential. The main disadvantage with this method is determining the effective surface thickness of the developed toner for determining charge to mass ratio (O'Brien, 1989).

6.5.2.4 Charge Measurement by Applying a Flying Voltage

This measurement device has a lower and upper electrode provided in parallel to face each other. A flying electric field application unit is used to apply a flying electric field voltage between the electrodes, which allows the developer to fly from the lower electrode to the upper electrode. The current flowing in the upper electrode is measured to determine the charge of the developer (Wada, 1996).

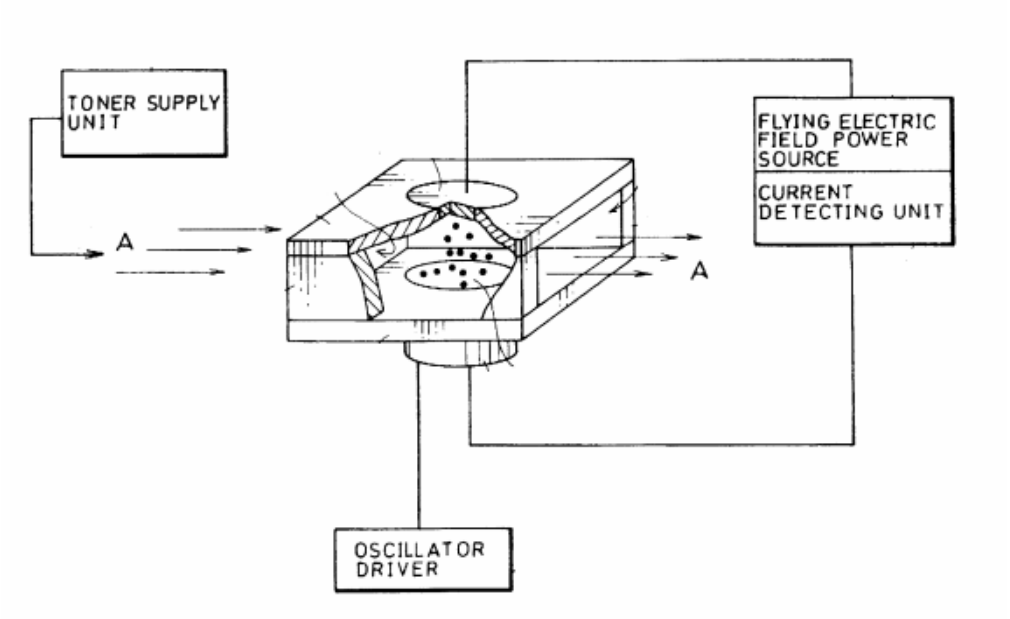

Figure 6-4 Charge Measurement by the Application of Flying Voltage

Source: (Wada, 1996), Sharp Kabushiki Kaisha (Osaka, JP)

6.6 Flow-ability

Toner flow properties play an important role in the development process. The triboelectric charging of toner depends on the friction between carrier particles and toner particles in a two component toner and friction between development roller and toner particles in contact charging of monocomponent toner. The toner particles must have good flow properties for uniform charging during the development process.

The height of the toner above the development roller in the development zone is limited by the doctor blade, and the toner particles must form a uniform layer without any surface distortion to present itself to the uniformly charged latent image in the photoreceptor. The toner must also exhibit good flow properties in spite of compaction by self weight in a toner cartridge. There are many factors that affect toner flow-ability, and they are explained in the following sections in detail.

6.6.1 Particle Shape and Size

Particle size and shape influence primarily the flow properties of the toner. In terms of shape, the main characteristic that affects its performance is the circularity of the powder. Circularity is defined as the ratio between the perimeter of a circle of equivalent area to the particle and the perimeter of the particle itself. Circularity can be viewed as an index of the degree of irregularities on the surface of a toner particle. So if the circularity were '1' then the shape would be perfectly spherical. As this value decreases, the surface shape becomes increasingly complicated. If the average circularity of a toner is less than 0.950, the toner particles tend to become coarse. Lower circularity reduces the flowability of the particles and produces trailing phenomena in the resulting fixed image. It also generates a wide variation in electrostatic charge from particle to particle, which impacts on the quality of that image.

6.6.2 Compaction

The toner powder may be compacted by its self-weight inside a toner cartridge. This property is known as caking. Toners having higher compaction index severely affect the charging operation due to more energy required for the toner powder to flow.

6.6.3 Attrition

The flow properties of toner powder are altered by attrition - the wear process that occurs when particles rub against each other or against containing surfaces. Particles may change in size and shape, become more rounded or more angular. Surface coating may be lost and the bulk density may be changed.

6.6.4 Aeration and De-aeration

Air is almost always present when powders flow, and not surprisingly, the amount of air can have a dramatic affect on the flow properties. An abundance of air may be present when toner particles are conveyed and at the other extreme, a stored powder may become consolidated with time as the entrained air is gradually excluded, or at least minimized.

6.6.5 Moisture Absorption

Exposure of a toner powder to atmosphere, particularly when the relative humidity is high, may result in moisture absorption and that will change the powder flow properties.

6.6.6 Bulk Density Dependence on Attrition

As mentioned earlier, the attrition of the toner particles may result in a change in bulk density due to the change in shape of the particles. The increase in bulk density may increase toner compaction.

6.7 Toner Flow-ability Measurement

There are different devices available to measure the flow-ability of toner. The determination of the flow-ability index by these devices are explained as follows.

6.7.1 Hosokawa Micron Powder Characteristics Tester

In this test, the toner is left in the ambient condition of 23° C and 60% RH for 12 hours, and 5 grams of the toner is accurately measured.

Sieve of 100 mesh (150 micron), 200 mesh (75 micron) and 400 mesh (38 micron) are overlaid in this order from top to bottom, and set on a shaking table. The accurately measured 5 g of toner is gently placed on the 100 mesh sieve, and gently actuated for 15 sec with an amplitude of 1mm.The weights of the toner powder remaining in the respective sieves are measured accurately.

The flow-ability index is calculated as

Flow-ability index (%) = A+B+C

A= (toner weight remaining in the 100 mesh sieve)/5

B= (toner weight remaining in the 200 mesh sieve)/5

C= (toner weight remaining in the 400 mesh sieve)/5

The application of the Hosokawa Micron powder characteristics Tester for measuring powder flow-ability measurement is cited by Kobayashi (1993).

.

6.7.2 Flow-ability Angle of Repose (ASTM C1444-00)

A funnel with a discharge spout opening of 0.25 inches to 0.38 inches with a capacity to hold approximately 0.25 lb to 0.5 lb is used to measure the angle of repose. The funnel is fixed to a stand, and a base plate is provided to collect the powder falling out from the

spout opening of the funnel. A reference height block of 1.5 inches is placed over the base plate and the tip of the spout is set to contact the reference block to set the right height between the base plate and the spout tip of the funnel. A stop is provided to cover the opening of the sprout. The internal diameter of the spout is measured to the nearest 0.01 inches. The stopper is inserted in the funnel and the funnel is filled with toner powder till it is nearly full. The stopper is removed, and the powder is allowed to fall freely on the base plate. The powder is fed into the funnel at the same rate as the powder is discharged from the sprout opening. The powder is fed to the funnel until the apex of heap cone formed by the powder reaches the tip of the sprout. The angle of repose is calculated as

$$\text{Angle of repose} = \tan^{-1}[2H/(D_A - d)]$$

where D_A is the base diameter of the cone, d is the diameter of the sprout and H is the height of the cone.

6.8 Monocomponent Toner Resistance Measurement

The resistivity of monocomponent toner is relatively low compared with the two component developers. The monocomponent toner electroconductivity and resistivity plays an important role, since the induced charge depends on the toner resistivity. Hence, it is important to control the toner resistivity within a desired range.

A small circular test cell with electrodes is used for measuring the toner resistivity. The toner is placed in a test cell between two brass electrodes of circular cross section, each with a cross sectional area of 0.073 cm^2. An insulating cylindrical sleeve made of polytetra-fluro-ethylene surrounds the toner and the electrodes such that the sample toner is constrained to the shape of a small pill box. At least one of the electrodes is free to move like a piston in the insulating sleeve to provide a predetermined compression on the sample. The compression is achieved by placing a known weight on the moveable electrode to give a pressure of 1370 g/cm^2 on the sample. Enough toner is placed in the

cell such that the final spacing between the electrodes is 0.05 to 0.1 cm and preferably as close as 0.05 cm. The final spacing is measured using a cathetometer. A voltage is applied in a series circuit arrangement consisting of the toner sample, an electric current meter and the voltage source. The toner conductivity is calculated from the voltage that appears across the electrodes and the current which flows through the closed circuit. The voltage is varied and the resulting conductivity is calculated for various fields from about 10 volts/cm to about 1000 to 4000 volts/cm. This measurement procedure is cited by Tabaru (1981).

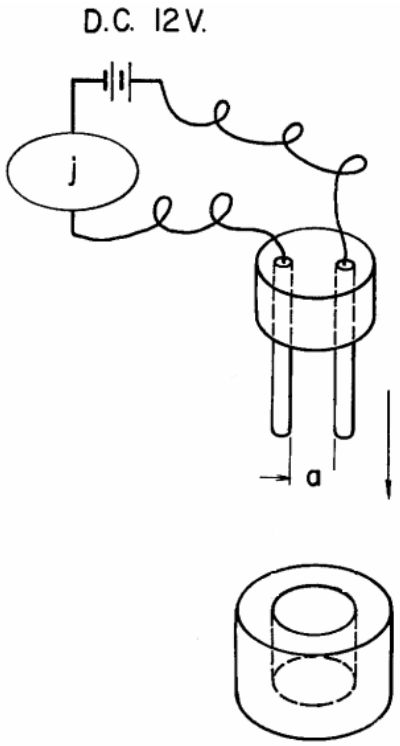

Figure 6-5 Device for measuring Toner Resistance

Source: Tabaru, (1981), Hitachi Metals, Ltd. (Tokyo, JP)

6.9 Dry Electrostatic Toner Fusion Temperature Measurement

The fusion point of a dry electrostatic toner is the temperature at which the toner starts to exhibit plastic flow. The fusion point is for a dry electrostatic toner is determined using a

microscope and micro hot stage device. The microscope has a 40 to 50 X magnification. The stage of the microscope is replaced with a micro hot stage that has a heater along with devices for precise temperature control and measurement.

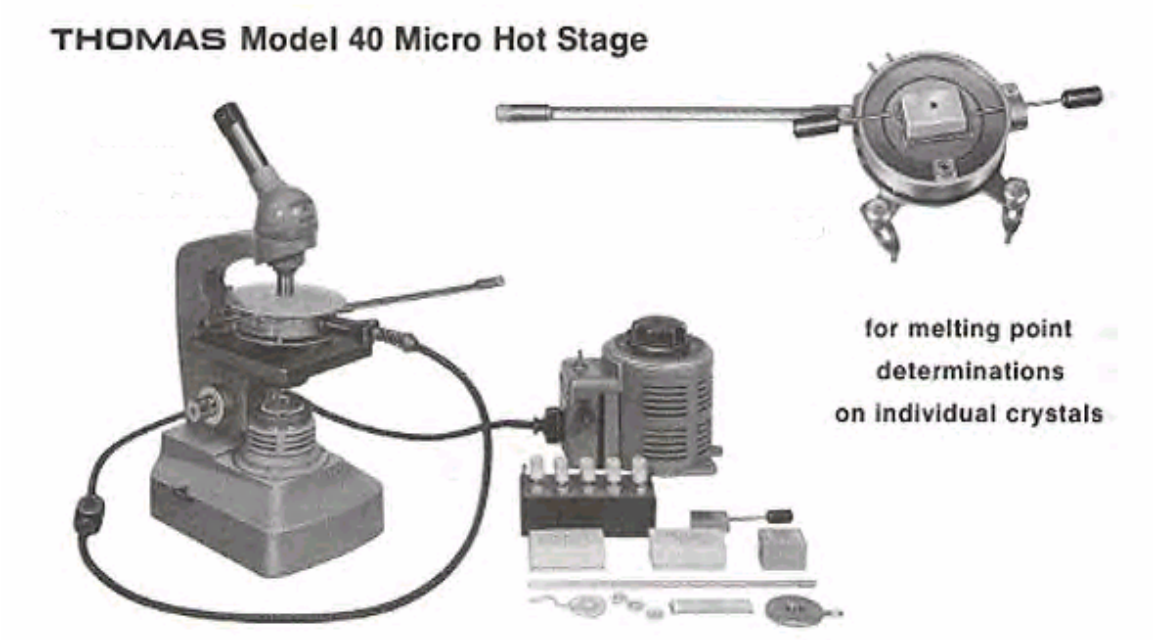

Figure 6-6 Microscope and Micro Hot Stage

Source: Aurther H Thomas: Manufacturer of Kofler Micro Hot Stage

Several grains of toner are transferred to a microscope slide using a spatula. The grains are accumulated in one spot to form a pile in the microscope slide. The toner is cover on top with a glass slide and is then placed over the micro hot stage. The microscope is then got into focus to reveal the sharp details of the particles in the slide. The micro hot stage is turned on and is set to heat at a rate of $3^{o}C$ till $10^{o}C$ below the expected fusion temperature. The rate is then adjusted to $2^{o}C$. The sample is observed through the microscope and the temperature is recorded when the fusion starts. The determination of fusing temperature of dry electrostatic toner is explained in ASTM standard F 706 - 96.

6.10 Caking Temperature of Dry Electrostatic Toner

Dry toners used in laser printers are normally free flowing powders at room temperatures. They are often formulated to fuse at elevated temperatures as part of the electrostatic printing process. The specific temperature at which fusing takes place has implications of premature change in the physical properties of a given toner, defined as caking or blocking. This is undesirable, but can result when the dry toner is subjected to temperatures in the range of its fusing point during conditions of transport, storage and local handling.

The caking temperature is determined using a circulating air oven with a temperature measurement device. Five grams of accurately weighed toner is spread in a round aluminum disc and placed in the circulating air oven. The circulating air oven is set at $40^{o}C$ for 24 hours. The discs are then removed from the oven and allowed to cool to room temperature. The toner in the disc is then stirred with a spatula to determine any evidence of caking. If there is any clumping then the blocking temperature is recorded as below $40^{o}C$. The same test is repeated in increments of $5^{o}C$ to determine any evidence of caking. If the sample does not cake at or below $80^{o}C$ then the blocking temperature is recorded as above $80^{o}C$. The standard practice of determining the caking temperature of dry electrostatic toner is provided in ASTM standard F 470 - 89.

6.11 Summary

The melting / kneading, suspension polymerization and spray drying processes for toner manufacturing were explained in details. The spherodization process for achieving the spherical shape of the toner particles was described. The process of triboelectrification for charging toner particles was explained in details along with the various materials present in the triboelectric series. The various property measurement techniques for determining the flow properties, particle size and shape measurement, charge , electrical resistance, fusion point and caking temperature were explained in great detail.

7 Experimentation

7.1 Introduction

The 3D laser printer uses a laser print engine for layer development. It is proposed to use a Teflon-coated fiberglass sheet as the receiving medium for the developed toner image from the photoreceptor of the print engine. The layer fixing in a laser printer is done by pressure temperature fusing. The same layer fixing concept is proposed to be extended for the 3D laser printer.

The proposed Teflon-coated fiberglass receiving medium and the pressure temperature fusing methods are to be evaluated for their suitability. The ability of Teflon-coated fiberglass as a receiving medium compared to paper used in the laser printer is to be evaluated by determining the weight gained by Teflon-coated fiberglass in comparison to paper after development. The 3D laser printer is under development in the Industrial Engineering department of NC state university. Researchers working on the development of the 3D laser printer are in the process of modifying the laser print engine for 3D laser printing. Since there is considerable work involved in the development of the print engine, alternative layer development techniques are considered to evaluate the effectiveness of the temperature-pressure fusing process.

A material testing station was developed to create and fuse toner layers similar to the operations in a 3D laser printer. The layering process is done by mechanical means. The fusing of the toner layers is done similar to the temperature-pressure fusing as proposed for the 3D laser printer. The material testing station simulates the operation of layer creation and fixing as in a 3D laser printer and thus provides a tool for evaluating the effectiveness of the layer fixing process.

The surface properties of the specimens can be evaluated to determine the suitability of depositing further layers for fixing. The strength of the specimen can be evaluated to determine the uniformity of the specimen.

The following sections provide details about the observations and experimentations done to analyze the effectiveness of layer development and fixing using a 3D laser printer.

7.2 Material Testing Station for 3D Laser Printer

The material testing station is used to test the feasibility of depositing polymer powders in a 3D laser printer. The polymer powders to be used in a laser printer must have good flow properties, consistent size and shape, proper electrostatic properties, and suitable thermal deformation properties. The development cost of a laser print engine is very high as it involves extensive experimentation to develop the right hardware and polymer powder material combination.

For this research, a material testing station was developed to identify the suitable material properties and to determine the feasibility of creating parts by layered manufacturing using a 3D laser printing. The material testing station was designed to simulate the layer development and fixing process required by a 3-D laser printer. The layer development is achieved by mechanical means and is not by electrostatic means as in laser printer. Hence, the electrostatic properties cannot be evaluated using the material testing station.

The material testing station was developed by retrofitting a CNC engraving machine. The tool spindle of the engraving machine was replaced with a container that holds polymer powder. The container with the toner moves along the X-axis of the machine spreading the toner uniformly across the bed. The container is capable of providing minimum height increments of 0.001 inches (25.4 microns), and thus layers of 0.001" height can be created for every pass of the container across the X axis.

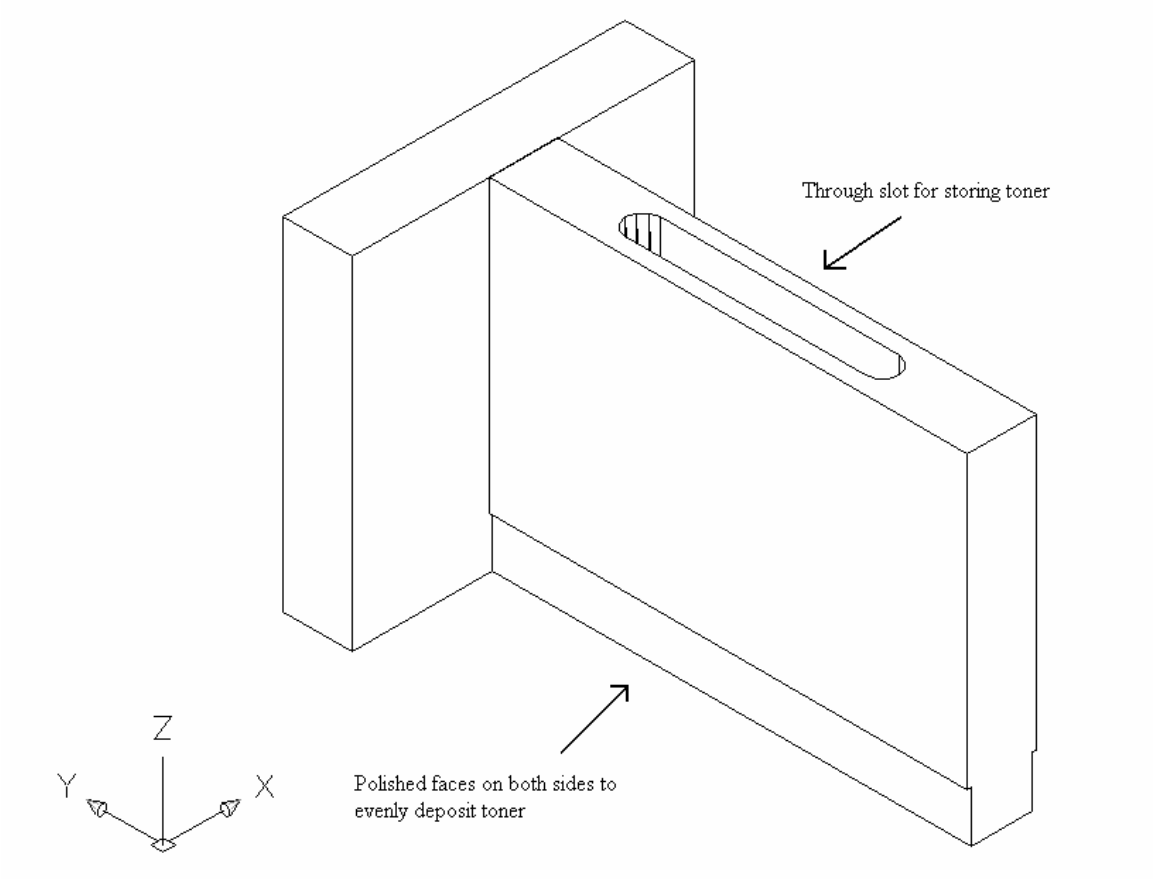

Figure 7-1 Toner container

The testing station has a heater that fuses the deposited layers by the toner container. The bed of the engraving machine has a bridge which contains the heater mechanism. The heater is made with a resistive heating element suitably housed in an aluminum block to provide uniform heating. The heater block is moved up and down to fuse deposited polymer layers using a pneumatic cylinder. The fusing time is precisely controlled using an Allen Bradly programmable logic controller, which reverses the pneumatic cylinder stroke after a specified time lapse. The temperature of the heater is controlled by an Omega proportional integral controller, which controls the temperature to a specified degree. The heater is wrapped in a Teflon-coated fiberglass sheet for fusing the polymer layers.

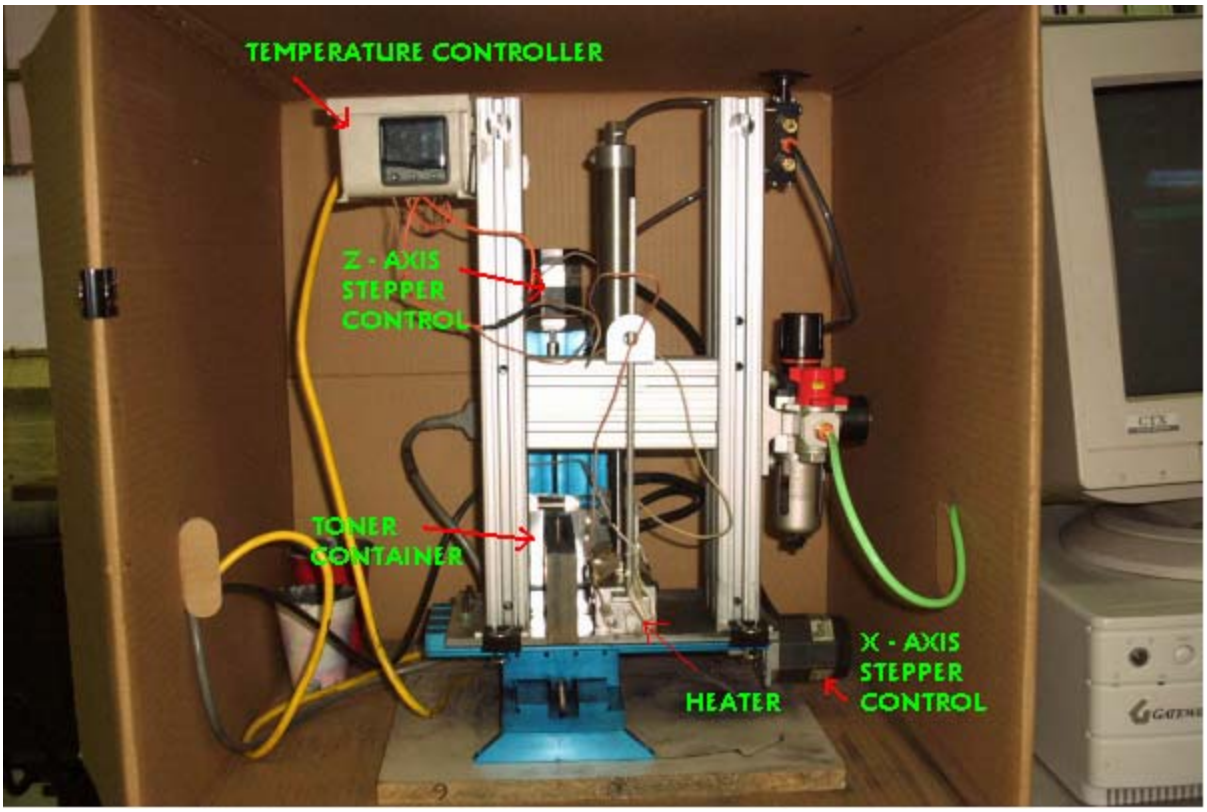

Figure 7-2 Material Testing Station

The force applied by the pneumatic cylinder used for the heater determines the heater-polymer layer contact pressure during the fusing process. The force applied by the pneumatic cylinder is precisely controlled using a load cell. The force of the pneumatic cylinder is changed by varying the excitation voltage of the SMC electronic pressure regulator.

The toner is deposited on a base plate which has ground parallel faces. The base plate has a layer of paper on the top to provide adequate adhesion to the deposited polymer layers. A layer of water-based adhesive is used before depositing the first layer to avoid peeling of the paper layer during the deposition and fusing of subsequent layers.

The material testing station was developed to simulate a 3D laser printer with a laser print engine. In a 3D laser printer, the layers of constant thickness are printed by the print

engine, and the layers are fused to the previous layers by the application of pressure and temperature. The application of pressure and temperature compresses the deposited layer, hence the final fused layer thickness is less than the deposited layer thickness. In the material testing station the exact process is replicated by depositing a toner layer of constant thickness with the container. The deposited layer is fused by the application of pressure and temperature, and subsequent layers are deposited over previously fused layers.

The fusing process for every layer is done by the application of pressure and temperature. The fusing process depends on the thermal deformation behavior of the toner, which is characterized by its glass transition temperature (T_g). The glass transition temperature divides the hard brittle regime from the soft, liquid or the flowing regime. The deposited toner particles in every layer are softened by the application of heat and are sintered together by the application of pressure. The contact geometry of two spheres in a sintering process (Frenkel, 1975) without application of pressure is given by.

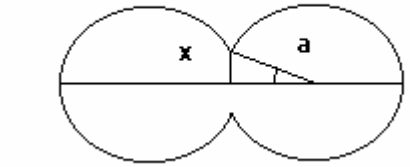

$$\frac{x^2}{a} = (\frac{3}{2})(\frac{\gamma}{\eta})t$$

Where γ is the surface energy in ergs/cm^2 and η is the viscosity in poise. From the above equation it is clear that the sintering process proceeds rapidly with low viscosity and high surface energy. The sintering process is enhanced by the application of pressure during fixing in the material testing station.

The viscosity of the polymer powder at glass transition temperature is approximately 10^{13} poise. The toner used in the material testing station had a glass transition temperature

near to 90° C. The glass transition temperature was approximated from the trial conducted for fusing the toner. The change in viscosity with temperature for a polymer powder with a glass transition temperature of 90° C is given by William Landel Ferry equation (Neilsen, 1977) as

$$\mathrm{Log}(\eta) = 13 - \frac{17.44 \cdot (T_i - T_g)}{51.6 + (T_i - T_g)}$$

where η is the viscosity in poise, T_i is the temperature in degrees Celsius or in Kelvin and T_g is the glass transistion temperature in degrees Celsius or in Kelvin.

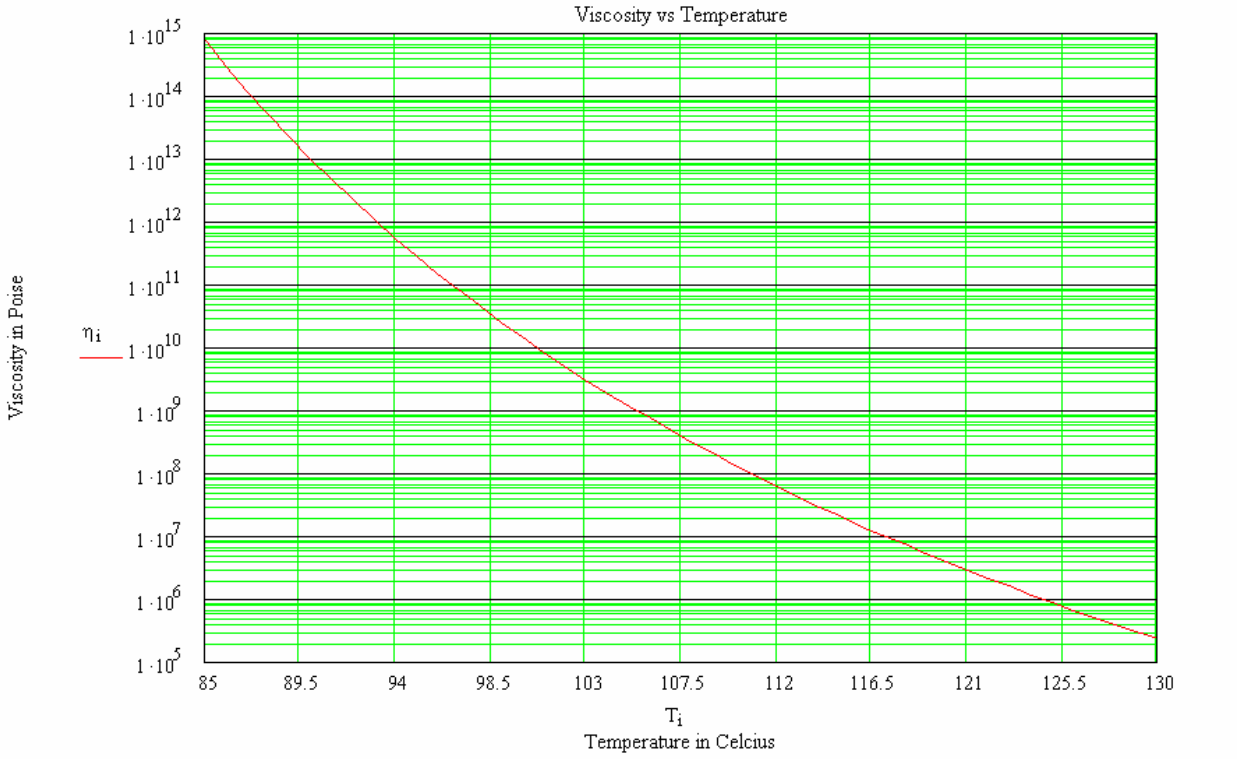

Figure 7-3 Viscosity Variation With Temperature for a Toner With 90° C Glass Transition Temperature.

The contact pressure applied for producing polystyrene-based HP4 toner specimens in the material testing station is 5.4 psi compared to the 130 psi contact pressure applied by the rollers in laser printing process. The temperature of the heater was set to 95^{o} C for the layer fixing process. The deposited layer is therefore softened due to heating and is fused with the previously deposited layer.

Based on the viscosity variation with temperature the creep rates during fusing are given by Maxwell's theory on creep of viscoelastic materials (Riande, 2000) as

Creep rate = Stress / Dynamic Viscosity

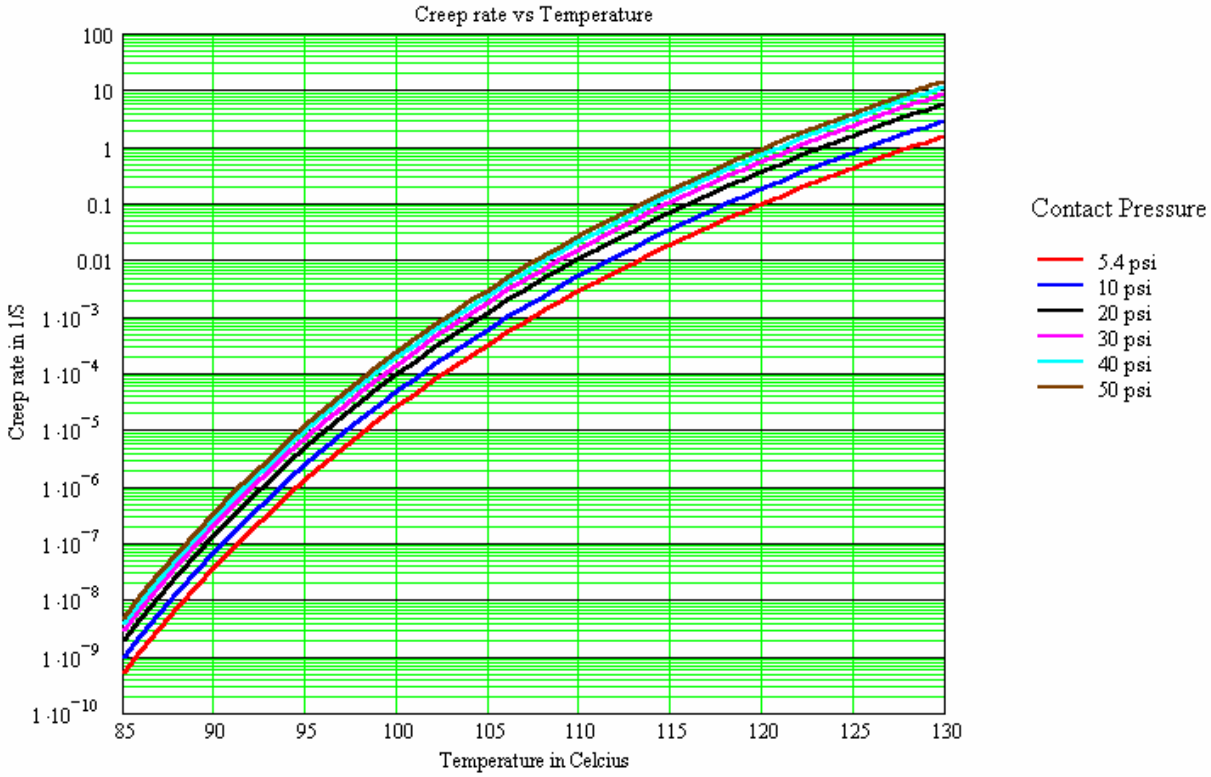

Figure 7-4 Variation of Creep Rate With Temperature for a Polymer a With 90^{o}C Glass Transition Temperature.

Figure 5-4 shows how creep rate is affected by variations in contact pressure. It can be observed that the creep rates are extremely low for a contact pressure of 5.4 psi and fusing temperature of 95 ^{o}C.

The container is capable of providing a height increment of 0.001" to deposit a layer thickness of 25.4 micron for each pass. The compression ratio (ratio of layer thickness after fusing to deposited layer thickness) of 0.75 is assumed after fusing for calculation purposes to explain the layering process. Due to the compression of the layer during the fusing process, the subsequent layer thickness deposited by the container is more than 25.4 microns (increment height of the container). It is observed that for container height increments of 25.4 microns and at an assumed compression ratio of 0.75, the deposited layer thickness stabilizes to 33.8 microns after just a few passes and remain constant thereafter. The fused layer thickness stabilizes to 25.4 microns, exactly to the value of the container increments and remains constant throughout the rest of the layering process. The fused layer thickness always stabilizes to the container increments irrespective of the value of the compression ratio used throughout the process. The layer developed in the material testing station is given by

$$\text{layer\_cumulative\_height}_{i+1} := \left(\text{container\_height}_{i+1} - \text{layer\_cumulative\_height}_{i}\right)\cdot \text{compression\_factor} + \text{layer\_cumulative\_height}_{i}$$

$\text{layer\_cumulatve\_height}_{i+1}$	-	Height of the deposited layer after fixing.
$\text{container\_height}_{i+1}$	-	Height of container during layer deposition
compression_factor	-	Ratio of deposited layer thickness to final fixed layer thickness.
$\text{layer\_cumulatve\_height}_{i}$	-	Height of the previously fixed layer.

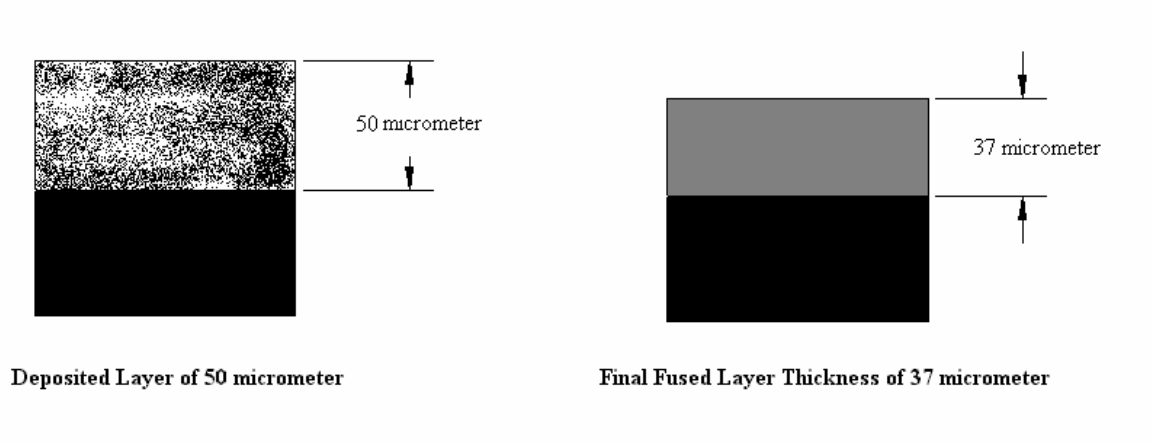

Figure 7-5 Layer Fusing in Material Testing Station

where the current layer height is given by the compression of the deposited layer thickness over the previously fixed layers. The compression ratio is expected to be precise for a given fusing temperature and pressure because of the uniformity in the size and shape of toner particles.

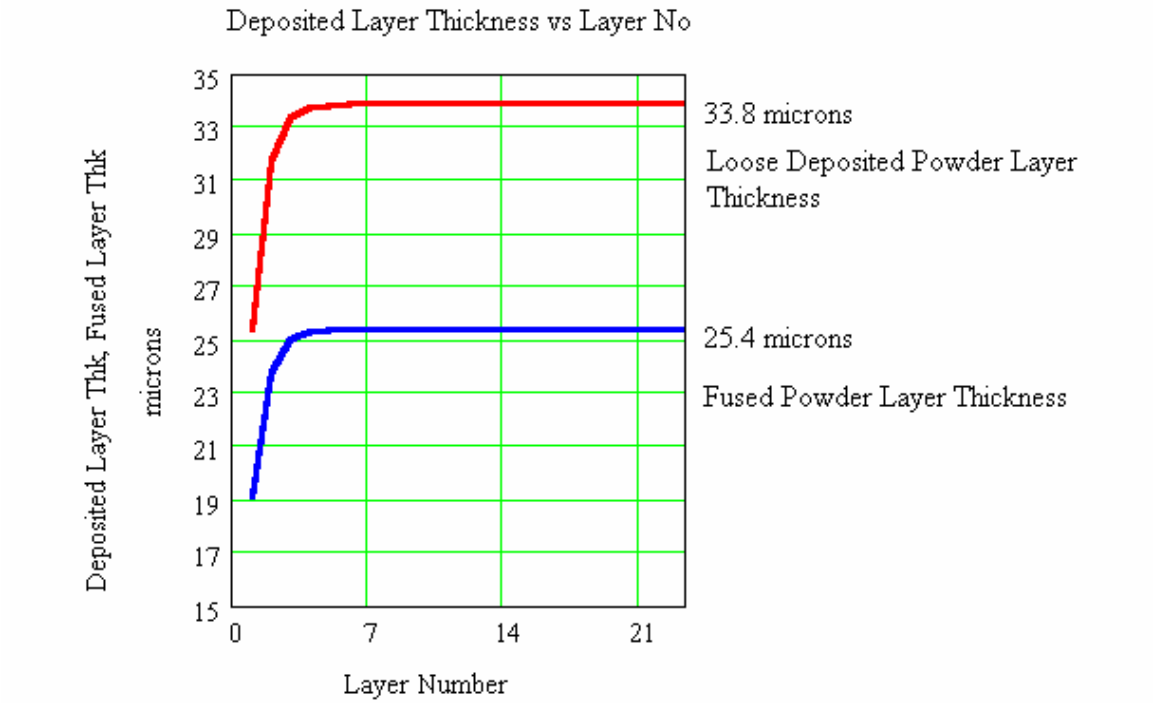

Figure 7-6 Layering in Material Testing Station

Based on the above analysis, the exact fused layer thickness can be obtained for a constant fusing temperature and contact pressure using the material testing station. The deposited layer thickness and the fused layer thickness for a given fusing temperature and contact pressure can be measured from the parts produced.

7.3 Tests Conducted Using the Material Testing Station

During the fusing process, the specimen may undergos thermal deformation resulting in a change in total specimen height. It is necessary to determine effects of thermal deformation on the specimen to determine the feasibility of producing parts by 3D-laser printing. Carslaw and Jaeger (1959) analyzed the conduction of heat through solids for pressure temperature fixing with paper and toner between the two rolls (Williams, 1984) They approximated the temperature at any point in the toner at a given depth to be

$$T(z,t) = T_0 + (T_s - T_0)erfc(\frac{z}{2(\alpha t)^{0.5}})$$

where z is the distance from the hot roll surface into the toner-paper combination, t is the fusing time in seconds, T_s is the hot roller surface temperature, T_0 is the temperature of the paper and toner before entering the hot roller, $\alpha = k/c\rho$ (cm^2/sec) is the heat diffusivity, k is the thermal conductivity (J/cm-sec-^oC) of the toner paper combination. c (J/g) is the specific heat and ρ (g/cm^3) is the density. The function $erfc(x) = 1 - erf(x)$ is a complimentary error function. The error function is given by

$$erf(x) = \frac{2}{\sqrt{\pi}}\int_0^x e^{-t^2}dt$$

The above model is used to determine the temperature of the toner layer thickness up to 300-micron thickness. The fusing temperature T_s was 95^o C and T_0 applied in the equation were 30^o C. The thermal conductivity of polystyrene is 1.172E-3 J/cm-sec-^{o}C and the specific heat is 1.339 J/g-^{o}C. The density of polystyrene is 1.05 g/cm^3. The

temperature distribution for a fusing time of 5,10,15 and 20 seconds from 1 to 300 micron toner depths is therefore given by

$$T_i := T_o + (T_s - T_o)\operatorname{erfc}(x_i)$$

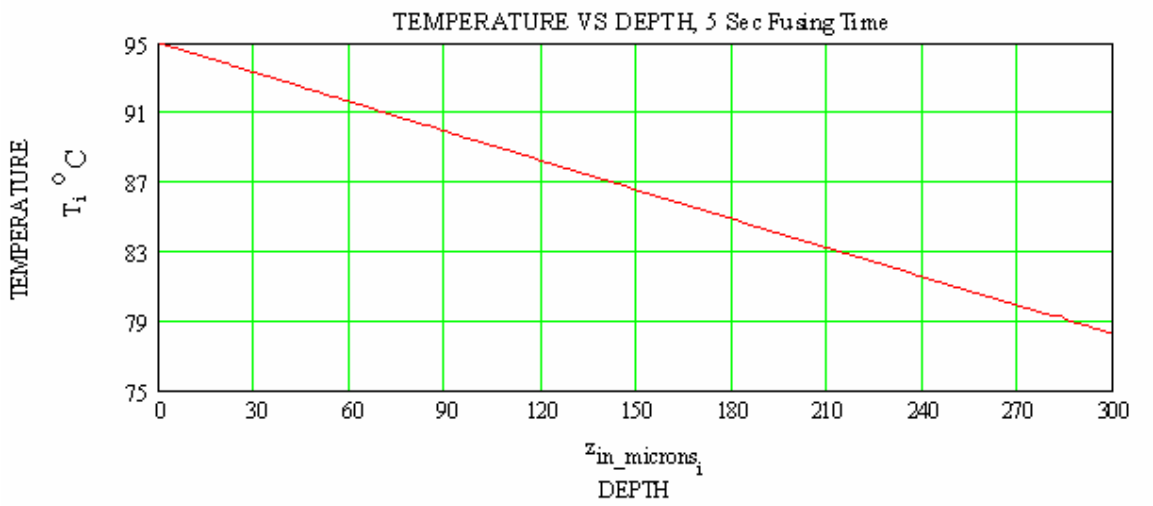

T_0-T_{300} = 16.74 C

Figure 7-7 Temperature Distribution Across a Depth of 300 microns for 5 second Fusing Time

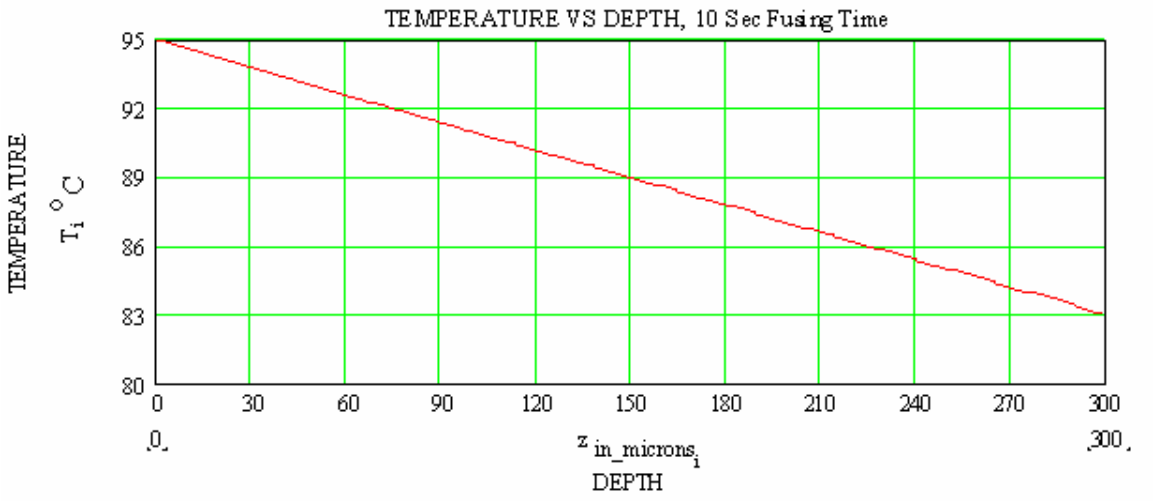

T_0-T_{300} = 11.94 C

Figure 7-8 Temperature Distribution Across a Depth of 300 microns for 10 second Fusing Time

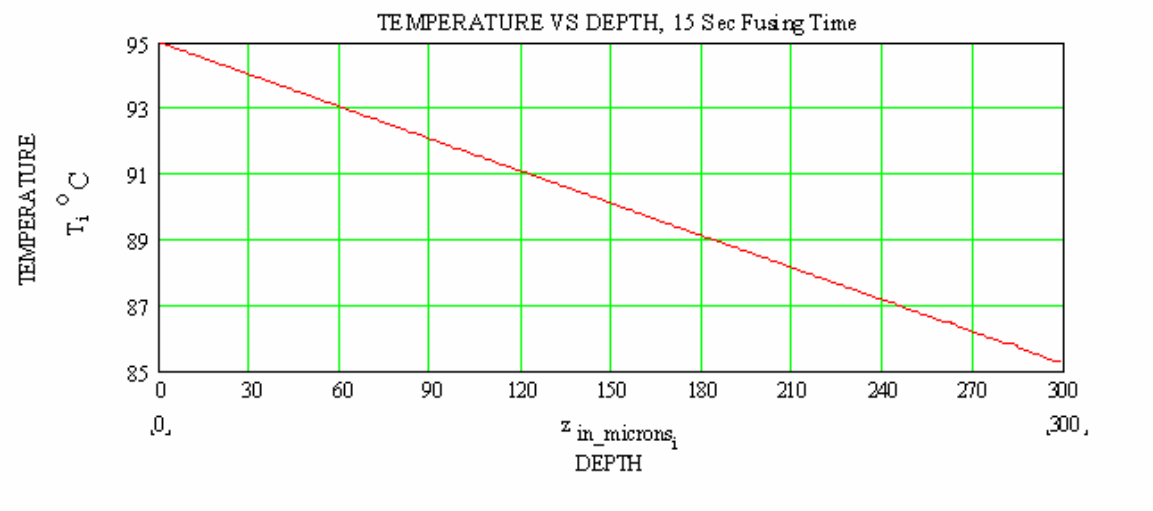

T_0-T_{300} = 9.78 C

Figure 7-9 Temperature Distribution Across a Depth of 300 microns for 15 second Fusing Time

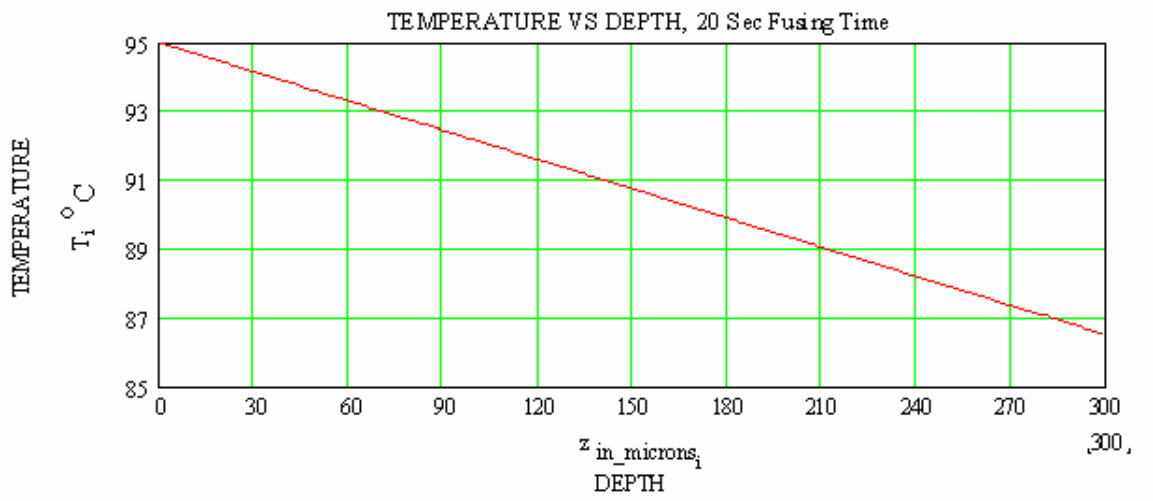

T_0-T_{300} = 8.48 C

Figure 7-10 Temperature Distribution Across a Depth of 300 microns for 20 second Fusing Time

It is observed that the temperature drop at a depth of 300 micron (20 second fusing time) is 8.5^{o} C. There is a region from the top surface of the specimen that is in a softened state due to the application of heat. If the thermal conductivity and specific heat of the powder polymer were comparable to that of aluminium (Specific heat - 0.90 J/g- C, Thermal Conductivity - 2.35 J/cm-sec-^{o}C) then the temperature at a depth of 300 microns will be 94.7 C in 5 seconds. This would results in more material being viscoelastic at higher depths from the top surface of the specimen. Hence, the lower thermal conductivity and higher specific heat of the polystyrene polymer contributes to the gradual propagation of heat unlike materials like aluminium.

During the fusing process the glass transition temperature is achieved at a depth of 175 microns from the top surface (Figure 5-10) after 20 seconds of fusing. The entire creep deformation takes place in the region where the polymer temperature is above the glass transition temperature. The total creep was estimated (Figure 5-4) for the depth of 175 microns for a contact pressure of 5.4 psi, fusing time of 20 seconds and 95^{o} C fusing temperature. The total creep was estimated to be 1.382E-3 microns for every fusing operation. This low creep can be attributed to the very high viscosity at glass transition temperature. The deposited layer will only undergo compaction due to pressure and the deformation due to creep must be negligible close to glass transition temperatures.

Hence, the low thermal conductivity and high specific heat of polystyrene polymer powder considerably reduces the viscoelastic region in the specimen. It is still essential to determine the extent of thermal deformation to determine the compensation to be provided in the deposited layer thickness. It is also important to assess the extent of thermal deformation to determine the feasibility of producing parts by 3D laser printing.

7.4 Evaluation of Thermal Deformation

7.4.1 Polymer Powder Material Used for Preparing the Specimen

The toner particles are classified based on size during the production process. The toner particles must have a form factor close to 1 and uniform size to attain good flow ability and uniform mass to area ratio during the layering process. Exactly 100 toner particles

were evaluated for size and shape using optical microscopy. The form factor (FF) is sensitive to variations in the particle outline and is given by

$$FF = 4\pi A / p^2$$

where A is the area and p is the perimeter of the 2D profile of particle viewed in the microscope.

A perfect circle has a form factor of one and the form factor provides a very good measure of particle roundness. The particle size can be measured by determining the Equivalent Circle Diameter given by

$$ECD = (4A/\pi)^{1/2}$$

The form factor and Equivalent Circle Diameter of 100 particles are provided in Tables 4.1 and 4.2

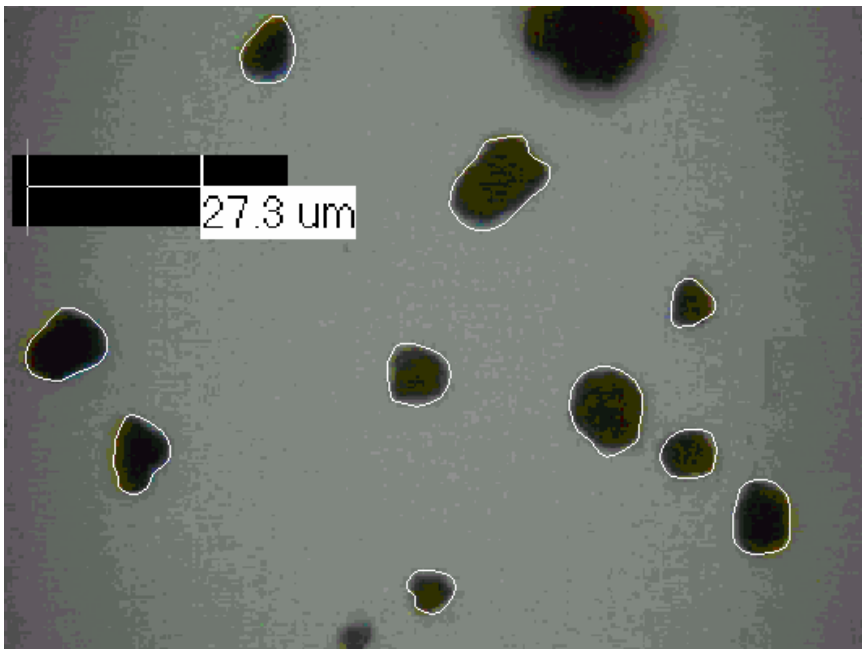

Figure 7-11 Particle Size Measurement by Microscopy

Table 7.1 Form Factor of Toner Particles

FORM FACTOR			Bin range			
		Bin No	From	To	Mean	Frequency
No	100	1	0.5830	0.6341	0.6085	1
Std dev	0.0892	2	0.6341	0.6851	0.6596	5
		3	0.6851	0.7361	0.7106	4
Scotts rule	8	4	0.7361	0.7872	0.7616	12
Sturges Rule	8	5	0.7872	0.8382	0.8127	10
Min	0.5830	6	0.8382	0.8892	0.8637	27
Max	0.9913	7	0.8892	0.9403	0.9148	24
Cell Width	0.0510	8	0.9403	0.9913	0.9658	17
MEAN FF	0.8595				SUM	100

Table 7.2 Equivalent Circle Diameter of Toner Particles

EQUIVALENT CIRCLE DIAMETER in microns			Bin range			
		Bin No	From	To	Mean	Frequency
No	100	1	6.1606	8.0693	7.1149	9
Std dev	2.9284	2	8.0693	9.9780	9.0236	22
		3	9.9780	11.8867	10.9323	25
Scotts rule	8	4	11.8867	13.7954	12.8411	25
Sturges Rule	8	5	13.7954	15.7041	14.7498	9
Min	6.1606	6	15.7041	17.6128	16.6585	5
Max	21.4303	7	17.6128	19.5215	18.5672	3
Cell Width	1.9087	8	19.5215	21.4303	20.4759	2
MEAN ECD	11.6370				SUM	100

It can be observed from the tables that the toner particles have a mean form factor of 0.86 and mean Equivalent Circle Diameter of 11.64 microns. It can also be observed that the particles have a narrow distribution of their size and form factor. The form factor of 0.86 illustrates the spherical nature of the toner particles and this is the reason for the higher flowability of these particles. The narrow distribution of the size and shape of toner

particles is also the reason for the uniform mass to area ratio attained during the solid area development.

7.4.2 Specimen Preparation

The form factor and the equalent circle diameter of the toner powder used for preparing the specimen was quantified in the previous section. The toner powder was used in the material testing station to create specimen and to analyze the fusing process of the toner layers. The toner powder was spread layer by layer by the container of the material testing station as explained in section 4.13.

The specimen was prepared by providing 0.001" increments to the toner container for every layer. The heater temperature was set to 95^{o}C and the contact pressure was set to 5.4 psi. The fusing time was set to 20 seconds. The operating parameters were determined by earlier trials in which two sample of 2 x 4 inch each with 74 layers was produced.

Figure 7-12 Seventy four Layer Specimen Prepared in Material Testing Station

7.4.3 Measurement of Thermal Deformation

The height of the specimen prepared in the material testing station was measured using a laser profilometer. The paper layer on the base plate was used as the reference for measuring the height of the specimen. The intial height of the specimen was used as the reference for measuring thermal deformation. After the intial measurement, the base plate with the specimen was loaded in the material testing station, and an idle pressing operation was performed with the heater set to 95^{o}C and 5.4 psi contact pressure. The fusing time was set at 20 seconds. The height of the specimen was measured again using the laser profilometer, and the amount of thermal deformation was quantified.

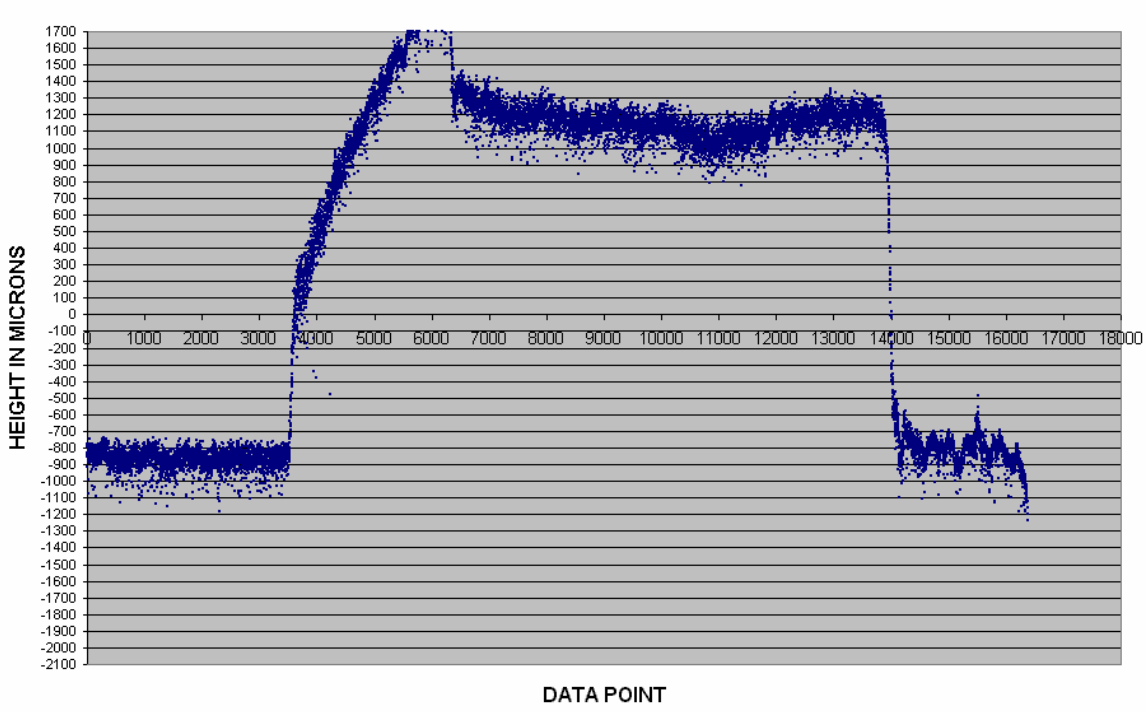

Figure 7-13 Specimen Height Measured by Laser Profilometer - 1

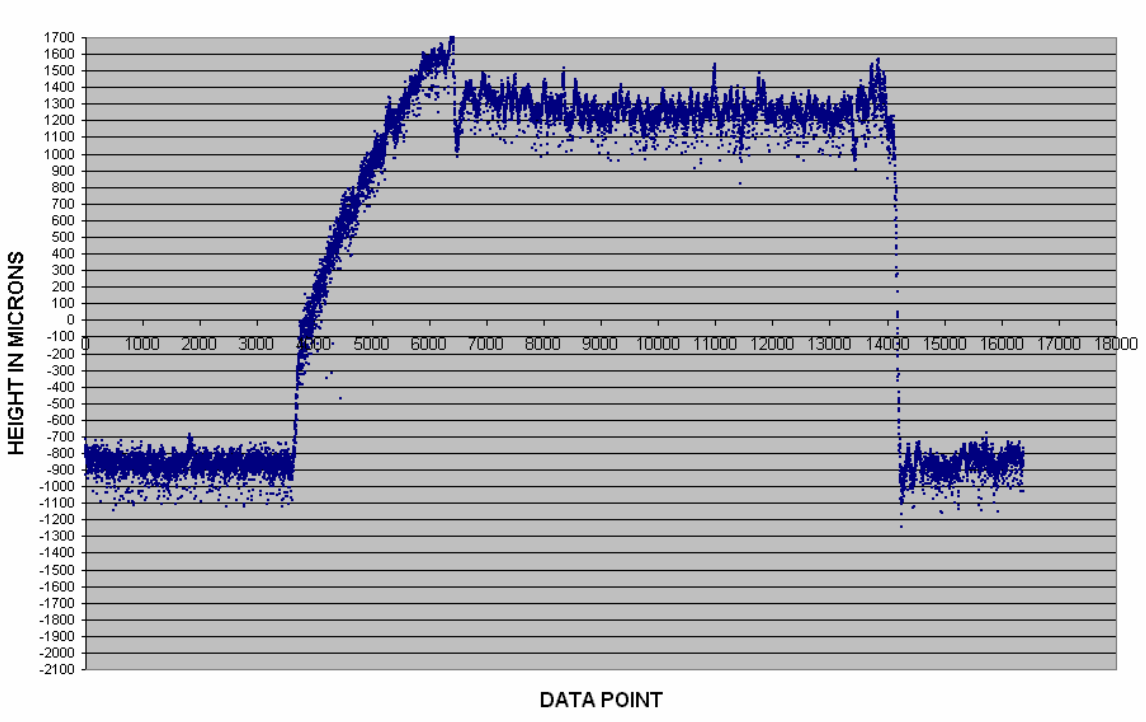

Figure 7-14 Specimen Height Measured by Laser Profilometer - 2

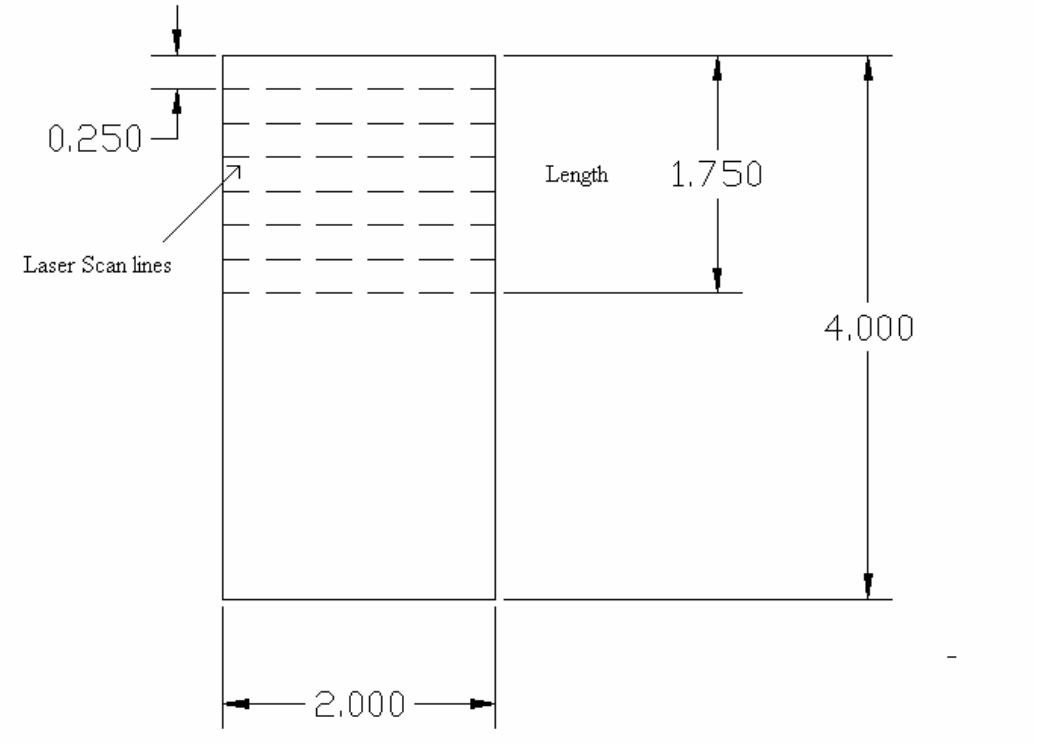

Figure 7-15 Laser Profilometer Scan Lines in a 2 x 4 Inches Specimen

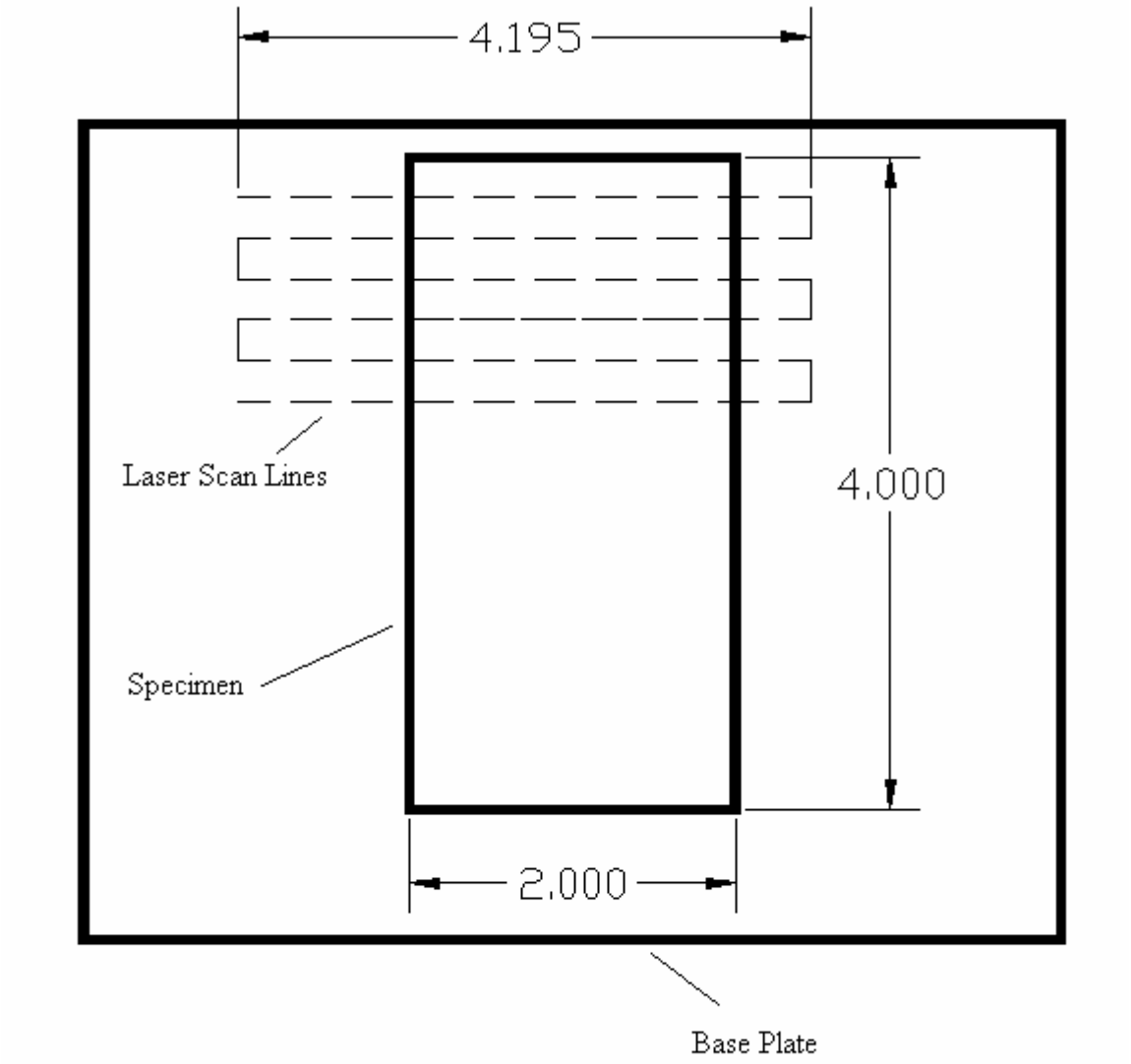

Figure 7-16 Laser Profilometer Scan Over Base Plate and Specimen

The data points measured by the laser profilometer have a spacing of 0.0003 inches. In a single pass of the laser, 16384 points are measured over a length of 4.915 inches (Figure 4-20). The specimen is deposited on a base plate. The base plate has a paper layer with a single toner layer of deposited by a laser printer. The data points 1 to 3000 (Figure 4-18) measures the surface properties of a single layer toner printed by a laser printer. The root mean square value of the surface roughness for data points 1 to 3000 is 53 micrometers. An insulating tape was used on one side of the specimen along the 4 inch length to prevent false trigger of the laser profilometer. The data points from 3000 to 8500 (Figure

4-18) represent the insulation tape and are discarded during measurements of specimen height. The data points from 9000 to 13000 provide the height reference and surface properties of the specimen. The surface roughness of the top surface of the specimen is 78 micro meter. The surface roughness is comparable to the toner layer deposited by a laser printer.

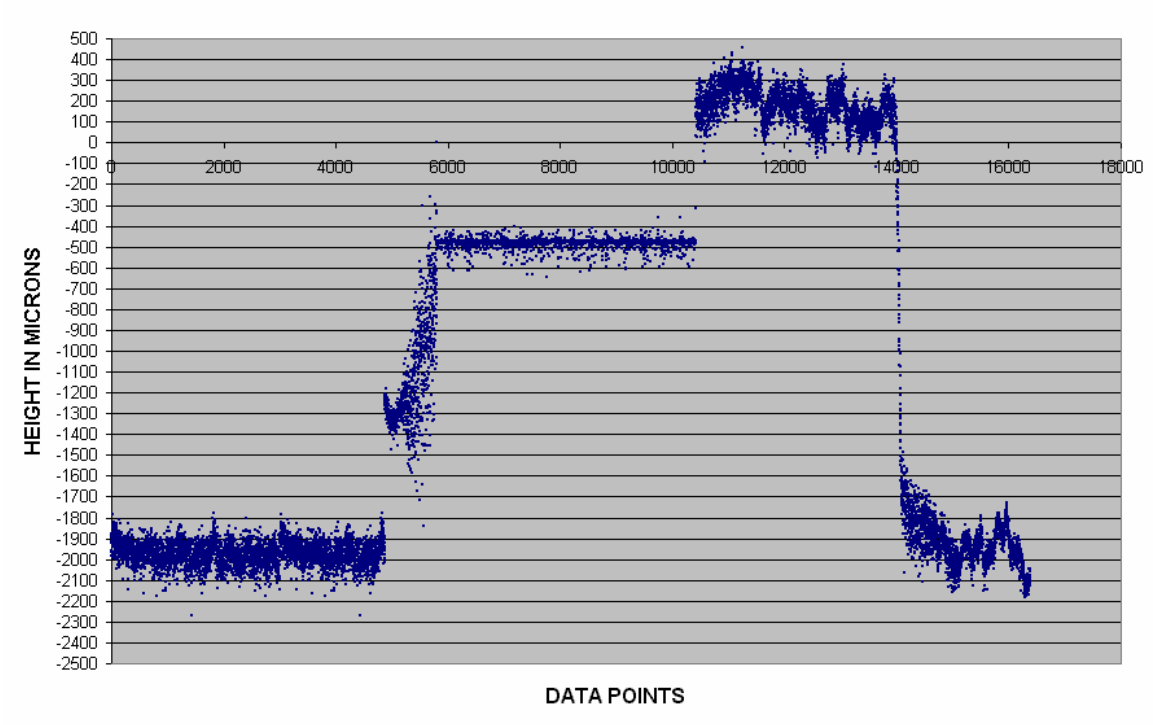

Figure 7-17 False Trigger Caused During Measurement

As mentioned earlier the height difference after a single press is measured over a length of 1.75 inches. The laser printer makes passes across the width of the specimen in increments of 0.25 inches. The measurements are as follows:

Table 7.3 Thermal Deformation of Specimen made in Material Testing Station.

No	Length Figure(4.19)	Height in micrometer Before compression	Height in micrometer After Compression	Decrease in Height (micrometer)
1	0.25	2122	2159	-37
2	0.50	2062	2066	-4
3	0.75	2041	2008	33
4	1.00	1997	1955	42
5	1.25	2161	2103	58
6	1.50	2162	2121	41
7	1.75	2129	2112	17
	Average Values	2096.28	2074.85	21.43

The average deformation over a length of 1.75 inches is 21.4 micrometer. The non uniformity in the decrease in height can be observed from the measurements. The decrease in height in the last 1.25 inches of 1.75 inches (Except for outliers 1 and 2) length is 38 micrometer. The specimens undergo slight warping at the edges due to uneven cooling taking place after fusion of the layers. Warping is a common occurrence with parts produced by different RP processes. The warping effect can be minimized by performing the fusing of layers with elevated ambient temperatures.

7.5 Shear Strength of the Specimen Prepared in Material Testing Station

In order to quantify the quality of fusing taking place, several shear specimens were prepared in the material testing station. The shear strength of the specimens were determined by testing six specimens of size 0.6 x 0.6 inches with a thickness of 0.135 inches, prepared from two of the larger 2 x 4 inch specimens made in the material testing station. A special test cell was made to gradually load the smaller specimens to shear failure (Figure 7-19). The specimens were secured in place between the jaws by tightening the screw fastener present in the jaws. A ram connected to a 0-100 lb load cell then gradually loaded the specimen to shear failure. The shear load on the specimen was gradually increased by increasing the air pressure of the pneumatic cylinder, which in turn was connected to the load cell and the ram.

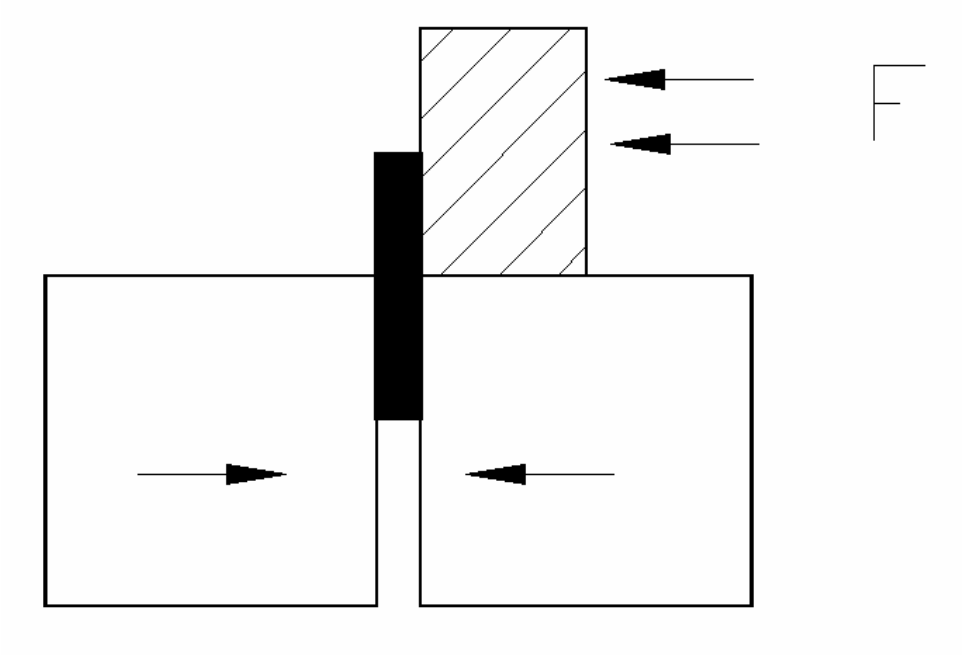

Figure 7-18 Gradual Shear Load Exerted on the Specimen in the Test Cell

The shear strength of the specimen were determined by testing six smaller specimens of size 0.6 x 0.6 inches with a thickness of 0.135 inches, prepared from two of the larger 2 x 4 inch specimens made in the material testing station. A special test cell was made to gradually load the smaller specimens to shear failure (figure 4-16). There are two jaws to secure the specimen and a load cell. One of the jaw slides on the dowel pins projecting from the other jaw. The specimen is secured in place between the jaws by tightening the screw fastener present in the jaws. A ram connected to the 0-100 lb load cell gradually loads the specimen to shear failure. The shear load on the specimen is increased by gradually increasing the air pressure of the pneumatic cylinder, which in turn is connected to the load cell and the ram.

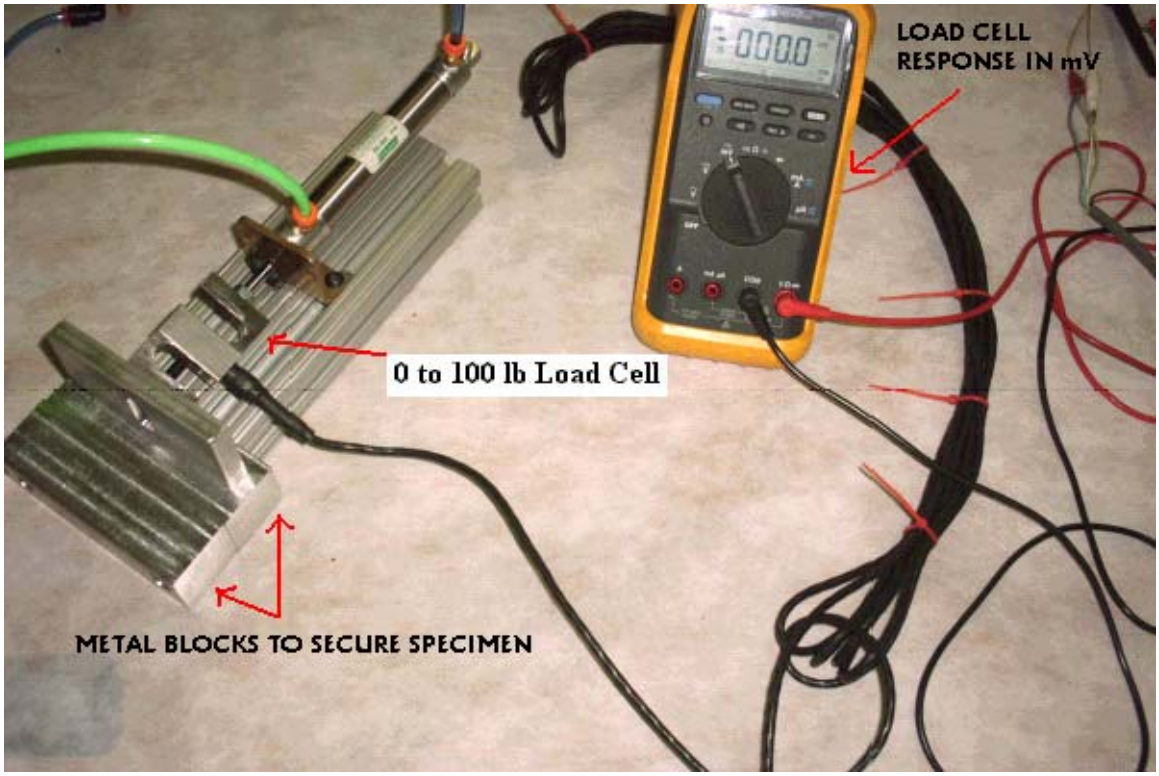

Figure 7-19 Test Cell for Shear Strength

Six specimens were tested for shear strength by gradual loading and the results are as follows:

Table 7.4 Results of Shear Test

No	Failure Load (lb)	Thickness (in)	Area (in^2)	Shear Strength (lb/in^2)
1	87	0.135	0.081	1074.07
2	70.1	0.135	0.081	865.43
3	89	0.134	0.0804	1106.97
4	94.3	0.139	0.0834	1130.70
5	84.3	0.139	0.0834	1010.79
6	84.2	0.139	0.0834	1009.59
			Average	1032.93

It can be observed that five of six specimens undergo failure at shear stress greater than 1000 lb/in^2 which was surprisingly high. It was quite evident that satisfactory fusion took

place at a 5.4 psi contact pressure, a 95^{o}C contact temperature, and a 20 second fusing time.

7.6 Variation in the Mass of Toner Deposited.

It is essential to have a uniform solid area development for printing layers using the print head in a 3D laser printer. The fusing process depends on the uniform mass to area ratio in the layers developed to achieve precise and repeatable fused layer thickness. In the following sections the consistency in layer development will be evaluated.

During 3D laser printing, layers are prefabricated in a 3D laser printer before the fixing process, and are fixed to other layers by thermal diffusion. The layers must have consistent regional densities to achieve uniform layer thickness and to obtain improved part accuracy and strength. There are approximately 200 million particles present in 10 grams of toner, and these particles have a specific size and shape distribution. It is therefore necessary to determine the regional mass to area ratio of the toner to determine the suitability of using laser printing for layered manufacturing.

The regional densities of toner were determined by printing a layer of toner on paper, and then determining the weight difference between equal cross sections of paper with a single layer of toner and clear paper at different regions. The cross section was a 2 inch circle obtained by shearing different regions of the paper with a single toner layer using a punching press. Thirty-two samples were punched to determine the mass to area ratio of the toner deposited. Out of the thirty-two samples, sixteen were single layer toner samples and sixteen were clear paper samples sheared at a different region of the same sheet of paper having a single toner layer. The results of the weight measurements are as follows:

Table 7.5 Measurement of Toner Samples to Determine Variation in Regional M/A Ratio

No	Toner sample	Paper Sample			
	(grams)	(grams)	Toner sample mean	Paper sample mean	Difference
1	0.1714	0.1548	0.1724	0.154225	0.018175
2	0.1734	0.1559			
3	0.1746	0.1551			
4	0.1702	0.1511			
			Toner sample mean	Paper sample mean	Difference
5	0.1715	0.1539	0.1694	0.1531	0.0163
6	0.1684	0.1542			
7	0.169	0.1502			
8	0.1687	0.1541			
			Toner sample mean	Paper sample mean	Difference
9	0.1677	0.1526	0.167775	0.152025	0.01575
10	0.1692	0.1525			
11	0.1676	0.151			
12	0.1666	0.152			
			Toner sample mean	Paper sample mean	Difference
13	0.1678	0.1519	0.167925	0.1506	0.017325
14	0.1688	0.1478			
15	0.1676	0.1506			
16	0.1675	0.1521			
SD	0.002273177	0.00211341			

The difference in mean for a 95% confidence interval between the single layer toner sample and the paper sample is expressed as follows:

Table 7.6 95% Confidence Interval for Weight Difference

	Toner sample	Paper sample
MEAN	0.169375	0.1524875
STDDEV	0.002273177	0.00211341
N	16	16
Z0	21.76335213	
Z ALPHA/2	1.962712	
95% CONFIDENCE INTERVALS		
Lower Limit in grams	Upper Limit in grams	
0.0154	**0.0184**	

The difference in mean provides the mass of the toner in the sample of a 2-inch circular cross section. It can be observed that the mass variation in a 2 inch circular cross section is very low. It is about 0.003 grams for a 95% confidence interval of difference in mean weights. This provides strong evidence that the 3D laser printing process is capable of producing very uniform layer densities. As mentioned earlier, the uniform mass to area ratio in the layer is essential for achieving precise fused layer thickness. The development process with the precisely engineered toner particles is consistent as proven by the results in Table 5.6.

7.7 Evaluation of Teflon as Good Receiving Medium of Polymer Powder

The receiving medium to be used in the 3D laser printer is a continuous fiberglass belt with Teflon coating. Teflon has good toner fixing properties without retaining residual toner. The receiving medium in a laser print engine is charged using a corona device for receiving toner from the latent image of the photoreceptor. It is necessary to determine if Teflon can be used as a good receiving medium. To determine the suitability of Teflon as a receiving medium, the heater mechanism in a print engine was disabled, and the amount of toner deposited on a paper was compared with the amount of toner deposited on a Teflon sheet for a given solid area. The results of the measurements are as follows

Table 7.7 Weight gained by Teflon Sheet

Receiving Medium	Weight Before Toner Deposition (grams)	Weight After Toner Deposition (grams)	Weight Difference (grams)	Average weight gained (grams)
Teflon 1	17.2553	17.3106	0.0553	0.04895
Teflon 2	13.3654	13.4080	0.0426	
Paper sheet 1	4.5725	4.6405	0.0680	0.07257
Paper sheet 2	4.6184	4.6910	0.0726	
Paper sheet 3	4.5618	4.6337	0.0719	
Paper sheet 4	4.6186	4.6934	0.0748	
Paper sheet 5	4.6026	4.6761	0.0735	
Paper sheet 6	4.5875	4.6609	0.0734	
Paper sheet 7	4.5521	4.6259	0.0738	

It can be observed from the above results that for a given solid area development, the weight of toner gained by a Teflon-coated fiberglass sheet is 67.4% of that which is gained by paper. This suggests that the Teflon-coated fiberglass belt is potentially a suitable transfer material for 3-D laser printing, but that the layer thickness needs to be compensated appropriately to account for the lower volume of material transfer. Thus far, the aim of 3-D laser printing process development efforts has been to use off-the-shelf print engines. It is worth noting, however, that the transfer efficiency of toner onto a Teflon-coated fiberglass belt can be increased by modifying the method by which the receiving medium is charged. The charging of the receiving medium with a corona device or by injection charging was explained in chapter 5.

7.8 Summary

The experiments and observations presented in this chapter prove that a part can be developed with the 3D laser printer by temperature-pressure fusing. The relatively low thermal conductivity and high specific heat of the toner material facilitates the layer development by temperature-pressure fusing. The toner particles are precisely engineered to have a narrow distribution of size and shape. The size and shape of the toner particles along with the consistent fusion point facilitates repeatability in fused layer thickness. It was demonstrated that a consistent mass to area ratio can be achieved with the printing process. A comparison of the transfer of developed image to paper and Teflon-coated fiberglass indicates that the coated fiberglass belt matterial can be successfully used as a receiving medium for developed images.

8 Conclusions and Recommendations

In the previous chapter, various observations and experiments were performed to determine the suitability of 3D Laser Printing as an RP process. A material testing station was constructed to help gain a better understanding of fusing process for a given polymer powder material. Specimens were constructed using the material testing station, and their thermal deformation during the fixing process was evaluated.

The measurements made using laser profilometers provided insight to the surface properties of the specimen constructed. The root mean square value of the surface roughness was determined to be 78 micrometers. The surface roughness of the layer fixed after depositing 70 layers is still comparable to the surface roughness of single toner layer produced by laser printing.

The deformation of the surface over a length of 1.75 inches was determined at a contact pressure of 5.4 psi, heater temperature of 95 degree celsius and contact time of 20 seconds. The mean deformation was determined to be 38 micrometers. In a 3D laser printer, the depth of the viscoelastic region can be reduced considerably by lowering the temperature and operating at higher pressures as depicted in Figure 5-4. It can be observed from Carslaw and Jaegers model (chapter 5) that the visco elastic region will be restricted to a very short depth of a few hundred microns resulting in minimal thermal deformation during the fixing process. It can be safely assumed that the specimens can be constructed with layers of precise mass to area. It is also suggested that the specimen be preheated during the layer fusing process to minimize the effect of warping.

The ability of the laser print engine to print layers with consistent regional mass to area ratios were demonstrated in Section 5.4. The minimal variation in regional mass to area ratios proves that there is a consistent layer development mechanism available for 3D-Laser Printing. Direct printing onto Teflon-coated fiberglass was successful, although the transfer efficiency was lower than that for plain paper. Nevertheless, the results indicate

that Teflon-coated fiberglass sheeting material is a candidate receiving medium to transfer toner from the photoreceptor (section 5.5). Thus a layer of toner with a precise mass to area ratio can be created and successfully fused with the previously deposited layers.

The polymer powder needed for making specimens can be modeled based on the toner used for laser printing. This provides a wide choice of materials that can be used for making prototype parts via 3D Laser Printing. The shear strength of the specimens made with toner powder was tested by gradually loading the specimen to shear failure. The specimens were found to have consistent strength at different regions. The specimens were able to withstand higher shear loads before failure.

The experiments performed till now prove the successful fixing of layers by temperature pressure fusing. Further experiments can be performed at higher contact pressures and reduced fusing temperature and time. The sintering of toner particles can be increased by increasing the contact pressure at a given fusing temperature and fusing time. This produces lower thermal deformation and lower warpage of the specimen during the fixing process. It is also possible to mount a laser profilometer device on the bridge of the material testing station to analyze the layers as they are created. This will provide an insight into the compression factors of the deposited layer during fixing.

Encapsulated toners are used in laser printing to protect the toner from the environmental effects of wear and tear. Encapsulated toners have a hard shell polymer containing a soft polymer core. Encapsulated toners are manufactured by spray drying or suspension polymerization as explained in section 4.2. The same concept can be extended to 3D laser printing by producing toner particles with hard core polymer having higher glass transition temperature and a suitably soft shell. The soft shell can be formulated with a lower glass transition temperature and will allow the fixing of deposited layer at lower compression ratios.

The concept of encapsulated toner particles can be extended to coating metal particles with polymers. Polymer-coated metal particles are already being used for carrier particles in insulative magnetic brush development (section 3.9.2). The carrier particles are 200 to 300 micrometer in size and have the capacity to retain charge in the polymer coating. The same concept can be extended to metal particles of smaller size comparable to the size of toner particles. The part can later be sintered in an oven to produce metal parts.

The experiments and conclusions discussed so far suggest that the temperature pressure fusing can be applied successfully to fix layers in a 3D laser printer. The 3D laser printer is still under development in the Department of Industrial Engineering at NC state University, and the studies performed so far can be successfully applied to the ongoing research.

9 References

ASTM F 577-83, "*Standard test method for particle size measurement of dry toner"*.

ASTM F 1877-98, "*Standard practice of characterization of particles"*.

ASTM C 1444 - 00, "*Standard test method for measuring the angle of repose of free flowing mold powders"*.

ASTM F 1425-92, "*Standard test method for determining the tribocharge of two-component developer material"*.

Allen, T. (1990). "*Particle Size Measurement"*

Borsenberger, P.M., Weiss, D.S. (1998). "*Organic Photoreceptors for xerography"*.

Carslaw, H.S. and Jeager, J.C (1959), "*Conduction of heat in solids"*, 2nd ed, Oxford at Clasrendon Press, Oxford.

Choi, A.Y.H. (1964), "J. *Appl. Phys"*.

Cooper, J. F. (1992). "*An Introduction to dry Toner Technology"*.

Dean, A., Castle, G.S.P, Schein, L.B., (1989). "*The effect of toner charge magnitude on magnetic and non-magnetic monocomponent development"*, The fifth international congress on advances in non impact printing technology, (editor) John Moore

Donald, D.K, Watson, P.K., (1970), "Photogr. Sci. Eng".

Edgar M. Williams (1993). "*The Physics and Technology of Xerographic Processes"*.

Frenkel. (1945), "*J. Phys"*. USSR

Genthe, James E., Buchan, William R. (1975), "*Cascade development station having a roughened development plate for enhancing developer mixture turbulence",* U.S patent 3, 991, 712.

James E, William R., Itek Corporation, "*Cascade development station having a roughened development plate for enhancing developer mixture turbulence".* U.S. patent 3,991,712, 1976.
Nakajima, J., Teshima, A, M. Horie (1980), "*Trans. Inst. Electron. Commun*. Eng". Jpn

Kamiyama, Masafumi, Maeda, Masahiro, Totsuka, Hiroki, Sano, Akihiro, Matsushita, Toshiya (1993), "*Suspension polymerization method and toner for electrophotography obtained therewith*", U.S. patent 5,346,798.

Kobayashi, Tetsuya, Fujii, Haruo, Katoh, Motoi, Kobayashi, Tatsuya, Miyashiro, Toshiaki, Enomoto, Naoki, Uchiyama, Akihiko, Saito, Yoshiro (1993), "*Developing apparatus using one component toner with improved flowability*", U.S. patent 5,307,127.

Kumar; Samir, Tirado, Morales, J. A. (2000), "*Particulate smoothing process",* U.S. Patent 6,383,706.

Matkan, Josef (1980), "*Microcapsular electroscopic marking particles",* U.S. patent 4,307,169.

Moriya, Yuichi (1994), "*Magnetic Toner",* U.S. patent 5,561,018.

Nelson, Kerry S. (1976), "*Electrographic development process*", U.S. patent 4,121,931.

Neilsen, L.E., (1977), "*Polymer Rheology"*

O'Brien, Richard W. (1989), "*Determination of particle size and electrical charge*", U.S.patent 5,059,909.

Riande Evaristo, Ricardo Diaz-Calleja, Margarita G. Prolongo, Rosa M. Masegosa, Catalina Salom (2000), "*Polymer Viscoelasticity, Stress and Strain in Practice"*, Marcel Deckker Inc., New York.

Ryne C. Allen (2000), "*Triboelectric Generation:Getting Charged"*, Desco Industries Inc. (DII)

Schein, L,B. (1992). "*Electro-photography and Development Physics"*.

Schein, L.B. (1974), "*In Electrography"*, Second International conference, (editor) White, D.R., (SPSE, Washington, D.C. 1974)

Schein, L.B (1975), "*Photogr. Sci. Eng"*.

Sullivan, W.A., Thourson, T.L. (1967), "*photogr. Sci. Eng"*

Tabaru, Kazunori, Aoyama, Takafumi, Kumakura, Toshio (1981), "*Preparation method of magnetic toner",* U.S. patent 4,482,623.

Van Engeland, J. (1979), "*Photogr. Sci. Eng"*

Williams, E.M. (1984), "*The physics and Technology of Xerographic Processes"*.

Wada, Takasumi, Yamamoto, Yoichi, Taniguchi, Keiji (1996),” *Measuring device for amount of charge of developer*”, U.S. patent 5,797,062.

10 Appendix A Equations for Layering Process

Analysis of Deposited Layers Date : 2/18/02

Initialize layer Count

$i := 1 .. 70$

$increment_i := i$

Container Increment height

$increment\_height := 25.4$

Container Height Position

$container\_height_i := increment\_height \cdot increment_i$

$container\_height_{71} := container\_height_{70} + increment\_height$

Deposited Layer compression factor

$compression\_factor := 0.75$

Final Layer Height Achieved

$layer\_intial\_height := increment\_height \cdot compression\_factor$

$layer\_intial\_height = 19.05$

Layer Thickness achieved after fusing

$$layer\_thickness_1 := layer\_intial\_height$$

$$layer\_thickness_{i+1} := \left(layer\_cumulative\_height_{i+1} - layer\_cumulative\_height_i\right)$$

$$mean(layer\_thickness) = 24.93$$

Layer Thickness before Fusing

$$Deposited\_layer\_thickness_1 := increment\_height$$

$$Deposited\_layer\_thickness_{i+1} := \left(container\_height_{i+1} - layer\_cumulative\_height_i\right)$$

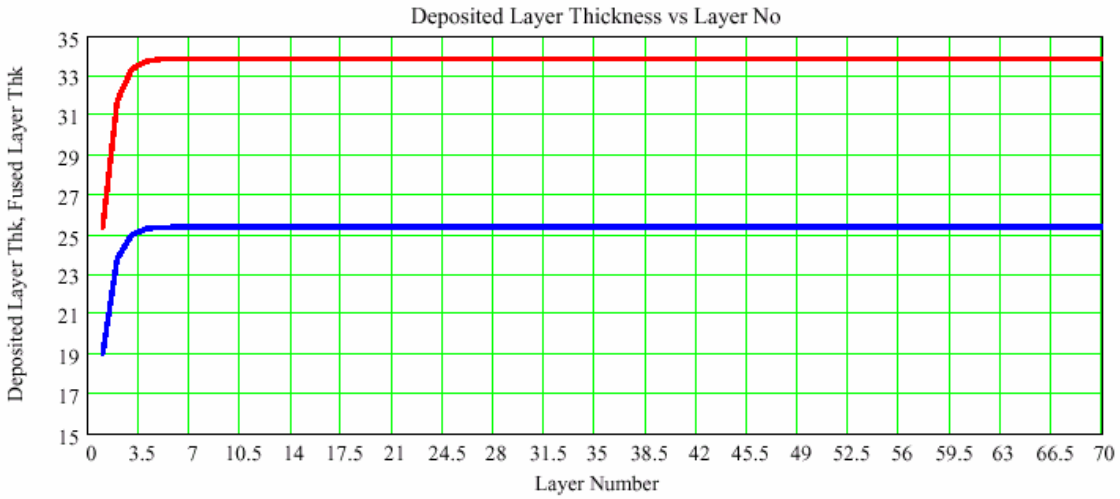

11 Appendix B Carslaw and Jaeger's Time Dependent Model

Carslaw and Jaeger's Time Dependent Model

Paper and Toner Initial Temperature in deg C

$T_o := 30$

Paper and Toner Initial Temperature in deg C

$T_s := 95$

Contact time in seconds

$t := 20$

$i := 0 .. 300$

Toner Layer Depth from the heater surface in Microns

$z_{in\_microns_i} := i$

Toner Layer Depth from the heater surface in centimeters

$$z_i := \frac{z_{in\_microns_i}}{10000}$$

Thermal Conductivity in J/cm-sec-C

$k := 2.8 \cdot 4.184 \cdot 10^{-4}$

Specific Heat in J/g-C

$c := 0.32 \cdot 4.184$

Density in g/cm^3

$\rho := 1.05$

Thermal Diffusivity in cm^2/sec

$$\alpha := \frac{k}{c \cdot \rho}$$

$$x_i := \frac{z_i}{2 \cdot (\alpha \cdot t)^{0.5}}$$

Temperature at a given depth in deg C

$$T_i := T_o + (T_s - T_o)\,\mathrm{erfc}(x_i)$$

$T_0 - T_{300} = 8.484$